BIONETS

WP 2.2 – PARADIGM APPLICATION AND MAPPING

D2.2.10 Advanced applications of game theory, electromagnetism and statistical physics

Reference:	BIONETS/INRIA/wp2.2/2.0
Category:	Deliverable
Editor:	Merouane Debbah (INRIA)
Authors:	Eitan Altman (INRIA), Rachid El-Azouzi (INRIA), Hamidou Tembine (INRIA), Yezekeal Hayel (INRIA), Merouane Debbah (INRIA), Gerasimos Pollatos (NKUA), Sophia Tsakiridou (NKUA)
Verification:	Daniele Miorandi (CN), Giusi Alfano (Supelec), Romain Couillet (Supelec), Samson Lasaulce (CNRS), Paolo Dini
Date:	August 19, 2010
Status:	Final
Availability:	Public

SUMMARY

The document is concerned with advanced applications of game theoretic, electromagnetic and statistical physics tools to the BIONETS architecture, protocols and services . It has both theoretical contributions (with new fundamental results derived) as well as practical implication designs. The deliverable contains 3 chapters; one on game theory, one on electromagnetism and one on statistical physics. We describe in the deliverable a rich number of fundamental contributions as well as actual scenarios in wireless networks that make use of them.

In chapter 2, a large population of players in which frequent interactions occur between small numbers of chosen individuals is studied though the use of the mean field approach. The second part takes a stochastic approach to model the game with individual states and establishes the existence of a stationary equilibrium. The third part formulates the placement of content to fixed nodes as a strategic game and provides conditions for achieving pure equilibria. Finally, the fourth part focuses on competition and cooperation mechanisms between nodes in Delay Tolerant Networks with Two Hop Routing.

In chapter 3, an electromagnetic approach nick-named “magnetons” is proposed to understand the routing of information when taking into account the mobility of the nodes. Extending previous works for fixed nodes (using tools of electrostatic), the optimal information flow is derived. The first parts describes the main tools of magnetostatics used whereas the second part focuses on the applications with various mobility models.

In chapter 4, statistical physics and random matrix theory tools are developed to characterize the spectrum of random Vandermonde and spiked random matrices. New fundamental results on the spectra of both type of matrices are derived. The case of random Vandermonde matrices turns out to be a useful framework for information retrieval and optimal deployment analysis of T-nodes. The applications are provided in the first part. The second part develops a cooperative T-node detection algorithm using spiked random matrices. The optimality of the algorithm is analyzed using large deviations.

Contents

Contents

DOCUMENT HISTORY

Version History

Version	Status	Date	Author(s)
0.1	Draft	24 June 2009	Mérouane Debbah
1.0	Final	30 August 2009	Mérouane Debbah
2.0	Revised	18 August 2010	Eitan Altman

Summary of Changes

Version	Section(s)	Synopsis of Change
0.1	ToC	Added
1.0	All	Added and aligned
2.0	3.3, 5	Revision to account for ESR comments

1 Motivation and Relevance

In the design and analysis of wireless networks such as those considered in BIONETS, researchers frequently stumble on the scalability problem. In other words, as the number of nodes in the network increases, problems become harder to solve. For example,

- *Routing:* As the network size increases, routes consist of an increasing number of nodes, and so they are increasingly susceptible to node mobility and channel fading.

- *Scheduling transmissions:* The determination of the maximum number of non-conflicting transmissions in a graph is a NP-complete problem.

- *Capacity*: As the number of nodes increases, the determination of the precise capacity region becomes an intractable problem.

Nevertheless, when the system is sufficiently large, one may hope that a macroscopic view would provide a useful abstraction of the network. The properties of the new macroscopic model would however build on microscopic considerations. Indeed, we may sacrifice some details, but this macroscopic view will preserve sufficient information to allow a meaningful network optimization solution and the derivation of insightful results in a wide range of settings. Quite remarkably, BIONETS-like systems are adapted to this scenario as they are self-adapting decentralized complex systems, where the interactions between T-nodes and U-nodes are quite difficult to model by means of classical tools.

Developing a systematic and principled approach for achieving this goal is the main theme of this report, and is firmly grounded in nature-inspired paradigms. We focus mostly on physics-inspired paradigms that exploit tools that have been developed to study inherently dense, disordered and decentralized systems. The approach we propose is based on probabilistic techniques that have been devised independently in the Game Theory, information theory, computer science and statistical physics communities. The application of of these paradigms to the dynamic, constrained optimization of BIONETS-like systems is a radical departure from the approaches taken traditionally by the communications engineering communities and provide a new scientific methodology to tackle the difficult problem of efficiently designing BIONETS-like systems.

The report is purposely interdisciplinary. It relies on the belief that problems at this level of complexity can only be solved by joining forces across disciplines and relying on techniques that have been developed to tackle complex physical and mathematical systems, albeit of a somewhat different nature.

The remainder of this report is organized as follow. In Sec. 2 we present a set of game theoretical results that have been obtained in the context of BIONETS networks. In Sec. 3 a novel approach for modelling and analysing routing in large-scale dense mobile networks, inspired by magnetostatics results, is presented and discussed. In Sec. 4 novel results on the spectrum of random Vandermonde and spiked matrices are presented, together with their application to optimal deployment problems in BIONETS-like systems. Sec. 5 concludes the paper discussing the potential impact of the results obtained on the design of efficient BIONETS systems and pointing out promising directions for expansion of the novel research directions identified.

2 Game theory

2.1 Mean Field Interaction models and evolutionary games for networks

We consider evolving games with finite number of players, in which each player interacts with other randomly selected players. The types and actions of each player in an interaction together determine the instantaneous payoff for all involved players. They also determine the rate of transition between type-actions. This model with a finite number of players, called mean field interaction has become more complex to analyze when the number of players grows (because a huge action profile space is required to describe all the of players). Then taking the asymptotic as the number of players goes to infinity, the whole behavior of the population is replaced by a deterministic limit that represents the system's state or population profile, which is fraction of the population at each type that use a given action. Mean field interaction models have already been used in standard evolutionary games in a completely different context: that of evolutionary game dynamics (such as replicator dynamics) see e.g. [9] and references therein. The paradigm there has been to associate relative growth rate to actions according to the fitness they achieved, then study the asymptotic trajectories of the state of the system, i.e. the fraction of users that adopt the different actions. *Non-atomic* Markov Decision Evolutionary Games have been applied in [10] to firm idiosyncratic random shocks and in [8] to cellular communications.

We have applied these modeling techniques to wireless applications in [7] and were able to propose efficient solution methodologies.

Contribution and Challenges

In [5], we consider a large population of players in which frequent interactions occur between small numbers of chosen individuals. Each interaction in which a player is involved can be described as one stage of a dynamic game. The state and actions of the players at each stage determine an immediate payoff (also called *fitness* in behavioral ecology) for each player as well as the transition probabilities of a controlled Markov chain associated with each player. Each player wishes to maximize its expected fitness averaged over time. This model extends the basic evolutionary games by introducing a controlled state that characterizes each player. The stochastic dynamic games at each interaction replace the matrix games, and the objective of maximizing the expected long-term payoff over an infinite time horizon replaces the objective of maximizing the outcome of a matrix game. Instead of a choice of a (possibly mixed) action, a player is now faced with the choice of decision rules (called strategies) that determine what actions should be chosen at a given interaction for given present and past observations. This model with a finite number of players, called a mean field interaction model, is in general difficult to analyze because of the huge state space required to describe the sate of all players. Then taking the asymptotic as the number of players grows to infinity, the whole behavior of the population is replaced by a deterministic limit that represents the system's state, which is fraction of the population at each individual state that use a given action.

We study the asymptotic *dynamic* behavior of the system in which the population profile evolves in time. For large N, under mild assumptions , the mean field converges to a deterministic measure that satisfies a non-linear ordinary differential equation for under any stationary strategy. We show that the mean field interaction is asymptotically equivalent to a Markov decision evolutionary game. When the rest of the

population uses a fixed strategy u, any given player sees an equivalent game against a collective of players whose state evolves according to the ordinary differential equation (ODE) which we explicitly compute. In addition to providing the exact limiting asymptotic, the ODE approach provides tight approximations for fixed large N. The mean field asymptotic calculations for large N for given choices of strategies allows us to compute the equilibrium of the game in the asymptotic regime. We also derive several evolutionary game dynamics and learning-based dynamics such as generalized Smith dynamics, replicator dynamics, logit dynamics, Brown-von Neumann-Nash dynamics, Ray-projection dynamics etc. We give sufficient conditions for convergence to equilibria.

Finally, we apply our approach to study the interaction of numerous mobiles competing in a wireless environment. In particular, we consider a wireless networks, where the resources are receivers, base station or access points and where users interact because of interference, i.e., interfering users cannot transmit simultaneously. There is a collision if another user (mobile) transmits with a greater power level at the same range of the receiver. Motivated by the interest of evolving dense networks, game theory evolving was found to be an appropriate framework to apply in networks. We provide asymptotic analysis of spatial random access based on mean field interaction where interfering users share resources placed on a undirected graph using an Aloha-type access control. We consider several classes of users. Users are spatially distributed and the arrival processes around each vertex are assumed to be independent. The interactions between users are nonreciprocal in the sense that the set of users causing interference differ from the set of those suffering from these interferences.

We also present an example of a dynamic version of the Hawk and Dove problem where each individual has three energy levels. We derive the mean field limit for the case where all users follow a given policy and where possibly one player deviates. We then further simplify the model to only two energy states per player. In that case we are able to fully identify and compute the equilibrium in the limiting MDEG. Interestingly, we show that the ODE converges to a fixed point which depends on the initial condition.

2.2 Stochastic Population Games with individual independent states and coupled constraints

In [6], we study a multiclass stochastic population game model with individual states. We consider several large subpopulations (classes or groups) of players. Each player from each subpopulation is associated with a controlled Markov chain, whose transition probabilities depend only on the action of that player (individual state). Each player interacts with a large number (possibly infinite) of others players. It does not know the states of, and the actions taken by other players. There are payoff (called also fitness, reward, utility) functions (one per subpopulation) that depend on the individual state and actions of all players.

Contributions and challenges

We characterize and establish the existence of stationary equilibrium in the stochastic population game model with individual independent states with time-average constraints under ergodic properties. A probabilistic representation of $\varepsilon-$equilibrium for time-average Cesaro payoff is obtained in the general (non-)communicating stochastic population game under feasibility conditions. We apply this model to dynamic renewable energy-state dependent power control and access control in wireless networks.

In the battery model, players (which correspond to users, mobiles etc) have their own battery. The state of each battery is described as a Markov decision process (MDP). Several types (classes) of batteries and several modes of rechargeable batteries are considered (renewable energy: solar, wind etc). In the battery-dependent power control population game, a non-decreasing function of the signal to interference plus noise ratio (SINR) is used as the instantaneous reward of the user. An equilibrium is explicitly determined in that case and the equilibrium payoff is expressed as function of the stationary distribution associated to that equilibrium. This model offers us a new class of repeated games: *constrained repeated games with individual states and unknown horizon* in a large population. We show that this class of games has a constrained $0-$equilibrium under ergodic and Slater conditions respectively on each individual Markov chain and constraints.

2.3 Placement of content to fixed nodes for optimal availability

In a typical BIONETS system, static sensor nodes (T-nodes) produce data that are to be utilized by moving nodes (users) which are referred to as U-nodes. Due to various reasons (such as energy or cost limitations) and depending on the application scenario, the T-nodes are considered to be severely resource-limited and as such, their processing, storage and communications capabilities are considered to be very limited. Consequently, T-nodes do not relay their content to other T-nodes within range, but they only make it available directly to passing by U-nodes when the latter as within the T-node range. U-nodes can pass data they posses to other U-nodes upon encountering them. As a result, a U-node interested in certain T-node data can obtain it (a) by passing by the T-node that produced it, or (b) though an encounter with another U-node that happens to carry such data.

This initial (core) BIONETS data dissemination paradigm has been studied in the past and its performance has been understood. To enhance the data dissemination process, some extensions to the core BIONETS paradigm have also been considered, e.g., involving resource-full Static Storage Nodes or the support of Reverse P2P Network Middleware (see BIONETS D1.2.3). The presence of Resource-full static nodes placed at crossroads has been shown to enhance substantially the data dissemination process.

In the current work we consider an extension to the core BIONETS environment that also assumes the presence of static storage nodes. Unlike in the case of resource-full storage nodes considered before - where the focus was on proving the concept of data dissemination enhancement through the presence of static storage nodes - in the current work we take a more realistic, distributed and autonomic approach to it as it will become clear below.

In addition to the existence of the T-nodes producing the data and the U-nodes using and disseminating the data, a number of distributed, self-interested, static nodes - to be referred to here as S-nodes - are assumed to be present, aiming at providing a data disseminating service to the core BIONETS environment. The follow assumptions are made for these S-nodes:

- S-nodes are resource limited to some extent, but they are more powerful than the (typical) T-nodes. In this work we assume that the S-nodes can store up to a maximum number of T-node data objects; that is, they are storage limited.

- S-nodes are assumed to be self-interested, form collectively a distributed group (distributed storage

resource) for replicating collected T-node data, and have some (non-inexpensive) communication capability among them.

- S-nodes are fed by T-node data by the U-nodes passing by.
- S-nodes can provide T-node data to passing by U-nodes requesting them in two ways. If the S-node possesses the requested T-node data it provides it to the U-node at low cost (or at high benefit to the S-node). If the S-node does not possess the requested data, it can look for it and fetch it from some other S-node (if available anywhere in the group) and can provide it to the requesting U-node at a higher cost (of for a lower benefit to the S-node), assuming that the U-node is still within the S-nodes proximity.
- S-nodes gather statistics concerning the interests in T-node data of the passing U-nodes. Using these statistics each S-node i forms a vector R_i of all the requested T-node data objects and a vector of preferences (access frequencies) W_i for objects in R_i. These two vectors are continuously updated so that at each given time each S-node has an accurate *snapshot* of the current trends in the BIONETS system.
- S-nodes do not only passively collect data from passing U-nodes and provide them to other passing U-nodes requesting them. They are also able to reconfigure collectively - as a selfish replication group - data that they select (based on some benefit maximization criterion) to store in their constrained storage capacity.

For the rest, let cap_i denote the storage capacity of S-node i and let P_i denote its *placement*, i.e., the set of T-node data objects it currently replicates.

We consider a scenario under which, in pre-specified time intervals, the S-nodes collectively initiate a procedure to try to reconfigure their contents by exchanging information so that each one individually optimizes its own *benefit*. The *benefit* of each S-node, denoted by b_i, is defined as the negation of the sum of the access cost for all information objects o not belonging in P_i, that is $b_i = -\sum_{o \in R_i \setminus P_i} c_i(o)$. The cost $c_i(o)$ is simply the product of the requested object's o preference $w_i(o)$ multiplied by the lowest possible cost $d_i(o)$ of fetching the object from another S-node that holds the object. This reconfiguration procedure is initiated each time in respect to the union of the information objects that all S-nodes collectively replicate.

Since during the reconfiguration procedure each S-node tries to replicate content for its' own benefit - offer high availability of content to all U-nodes passing nearby - it is straightforward that the content of each S-node's local storage will be highly optimized individually for it (the S-node will act as a selfish agent). For the distributed storage group of S-nodes though, all placements together are highly unlikely to produce a socially optimum configuration of objects to S-nodes, that is, a configuration that optimizes the sum of all individual benefits.

A most suitable way to study this scenario is to formulate it as a strategic game ([41]) where S-nodes behave as rational agents as follows: the strategic game is defined by the triple $< N, \{P_i\}, \{b_i\} >$ in which N is the set of S-nodes and each S-node i is a player (from now on we will use the terms S-node and player interchangeably) with strategy space $\{P_i\}$ consisting of all cap_i-cardinality subsets of the set of its requested objects R_i, that i may choose to replicate in its storage. The utility of each player i is its benefit

b_i that it wishes to maximize. Thus, every placement X is a strategy profile for the formulated game. If we denote by $X_{-i} = \{P_1, P_2, \ldots, P_{i-1}, P_{i+1}, \ldots P_n\}$ the strategy profile of all players apart from i, then each player can determine it's *best-response* P_i to the other players' strategies X_{-i} by solving a suitable Knapsack ([43]) problem.

Our goal is to explore existence of equilibria in this strategic game. That is, existence of a strategy profile for all S-nodes under which no S-node has an incentive to choose a different replication strategy given the other S-nodes' strategies. At first glance the answer seems rather easy since game theory predicts ([41]) that each strategic game possesses mixed equilibria; these are equilibria achieved under a mixed strategy, that is a strategy according to which each player selects one of a combination of strategies to play with some probability.

The main drawback of mixed equilibria is that it is not easy to accept them as a description of the behavior of rational agents in a distributed system (see [44] or [41] for an extensive discussion). A rational agent would more likely take a deterministic decision, by playing a single strategy with probability 1 and alter it whenever it observes inefficiency throughout the system's lifetime (possibly not respecting the probability vector but the current situation in the network). Thus, we turn our attention on whether the formulated strategic game possesses pure equilibria, that is strategies for each S-node with probability one.

Independently of whether mixed or pure strategy equilibria exist (or are more preferable), the lack of coordination which is inherent in selfish decision-making will probably incur costs well beyond what would be socially optimum, i.e. the costs incurred if a central coordinating authority was present. This potential inefficiency is quantified by the standard measure of the *price of anarchy* (PoA) [38]. The price of anarchy is defined as the ratio of the cost of the worst possible equilibrium strategy profile over the socially optimum solution proposed by a central coordinating authority. However, there are situations where application-specific incentives might be used so that the system can reach a *better* or *preselected* more desirable equilibrium state. Inefficiency in these cases is measured using the *price of stability* (PoS) [37], [36]. The price of stability is the ratio of the cost of the best possible equilibrium strategy profile over the socially optimum solution cost. From a natural perspective, the PoA and PoS bound the worst and best possible behavior of a system, respectively, under selfish decision-making.

In [39], a preliminary study of the defined strategic game was conducted in the case where the topology of the induced subgraph of the S-nodes was a simple 3-level hierarchy ([40]) and all sensor data were assumed to be uniform-sized information objects. A distributed two-step algorithm was described that effectively resulted in pure equilibria states. In [42], these results were generalized in the case of multi-level hierarchies, whilst objects remained uniform-sized and preferences were binary. Furthermore, bounds on the prices of anarchy and stability were calculated.

In order to better capture the essence of the BIONETS environment we have to consider generalizations of the described setting that are most suitable for this dynamic environment. More specifically, we assume that S-nodes are placed arbitrarily over the system's geographical area, thus the underlying topology of the induced subgraph of the S-nodes has no special characteristics. Furthermore, the constraints of binary preferences and uniform-sized objects were dropped. From a theoretical aspect, the latter constraint allows for an NP-hard calculation in each player's best-response (since as noted before each such computation involves solution of an integer knapsack problem). By dropping this constraint, the resulting computation difficulty can be overcome using standard dynamic programming techniques and assuming that the storage

size of each S-node is not exponential when compared to the amount of the information objects.

The reconfiguration procedure amounts to a *standard* iterative best-response algorithm. In an effort to gain insight into the evolution of the costs of pure equilibria in comparison with the social optima, across varying parameters, we extracted empirical values for the prices of anarchy and stability as well as for the average ratio of coordination, which we define as the ratio of the average cost of all computed equilibria over the social optimum. The PoA, PoS and average ratio were computed from the worst, best and average equilibrium cost, respectively, that we observed over a large number of runs, randomly varying the initial object placements per S-node as well as the playing order of the S-nodes. In what follows we denote by $d_{\max}$ the maximum communication cost on the induced subgraph of the S-nodes and by $d_{\min}$ the minimum one.

In an effort to investigate how the system's performance is affected by the communication cost, in Fig. 1 we depict the extracted values for PoS, PoA and average ratio of coordination as $d_{\max}/d_{\min}$ increases. The sub-network in consideration consists of $n = 64$ S-nodes and a universe of 100 information objects. The topology is a complete graph with lowest communication cost $d_{\min} = 1$ and communication costs for all edges randomly chosen between $d_{\min}$ and an arbitrarily chosen large constant. Each S-node has $cap_i = |R_i|/2$ where $|R_i|$ is chosen randomly from the interval $[0,100]$. The request set for each one was constructed by uniform random sampling of $|R_i|$ information objects from the universe. That is, U-nodes passing by S-node i would request one of the $|R_i|$ T-node data with probability $1/|R_i|$. Object preferences for each S-node were drawn from a Zipf distribution with $\alpha = 0.5$. Two crucial observations can be made in respect to Fig. 1: (a) there is a significant decrease of the rate of growth of all ratios as $d_{\max}/d_{\min}$ increases and (b) the range of the different values of the ratios is rather narrow. The first observation essentially indicates that although the range of different communication costs becomes broader, achieved equilibria do not become *extremely* more expensive than socially optimum placements, thus the inefficiency due to lack of a central coordinating authority, stabilizes. The second observation indicates that in the formulated game all pure equilibria induce similar costs and thus there is no need to offer any incentives to the S-nodes so as to lead them to choose certain equilibria.

The practical independence of the values of the three ratios from the number of S-nodes is depicted in Fig. 2. Having chosen a fixed maximum communication cost, we gradually inserted S-nodes and measured the values of the three ratios. During the insertion process we maintained the maximum communication cost, that is we gradually modified the minimum communications costs with which an S-node could fetch and object from another S-node. The range of the extracted values is rather narrow, which indicates that the inefficiency of the system due to selfish decisions is independent of the number of agents (S-nodes).

The quality of equilibria when S-nodes differ in terms of the *activity* they exhibit in the distributed storage group, is depicted in Fig. 3. We define the activity of an S-node as it's demand ratio $q_i = \frac{|R_i| - cap_i}{cap_i}$. The demand ratio for the group is defined as $q = \max_i q_i$. The demand ratio for each S-node can also be interpreted as a measure of the frequency at which the S-node is contacted by U-nodes. Fig. 3 shows empirical values extracted for distributed storage groups of 64 S-nodes, where we chose 32 specific S-nodes and gradually increased their demand ratio (thus, increasing the demand ratio of the group). Our results indicate increasing values for the three ratios as the demand ratio increases. Since high values for the prices of anarchy and stability indicate inefficiency due to selfishness, we conclude that less frequently contacted S-nodes tend to operate in favor of more frequently contacted ones.

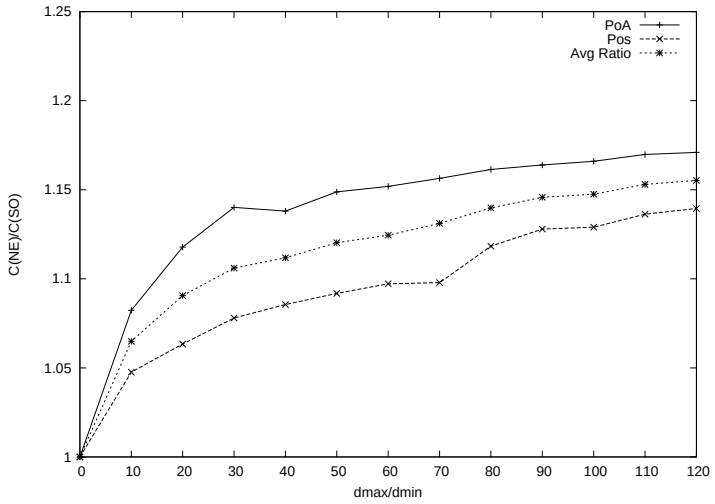

Figure 1: Evolution of PoS, PoA, and average coordination ratio (AVG) with $d_{\max}/d_{\min}$. $C(NE)$ is the cost of the Nash equilibrium while $C(SO)$ is the cost of the socially optimum solution.

Our results provide useful insight about the utilization of a self-aware distributed S-node environment in a BIONETS system. In terms of locating the S-nodes it suffices to choose locations such that $d_{\max}/d_{\min}$ is small, since the communication cost is the only parameter affecting the efficiency of the distributed storage group. Furthermore, the number of S-nodes present in the group, can be chosen without any consideration about the induced efficiency, since efficiency is independent of the number of S-nodes. What seems to be rather significant is how large the rate of requesting content from an S-node is, which is analogous to the frequency at which U-nodes contact an S-node. Even if a small number of S-nodes experience a high demand for T-node data, the efficiency of the distributed self-aware storage group can be substantially compromised. The latter potential loss of efficiency is worth exploring further and attempt to devise approaches that cope better with it.

2.4 Competition and cooperation between nodes in Delay Tolerant Networks with Two Hop Routing

Through mobility of devices that serve as relays, Delay Tolerant Networks (DTNs) allow non connected nodes to communicate with each other. Such networks have been developed in recent years and adapted both to human mobility where the contact process is between pedestrians, as well as to vehicle mobility.

DTNs have been in the center of BIONETS due to the very strong relation of DTN architecture to that of BIONETS, and due to the the way routing is performed in these networks, which can be modeled using standard tools in epidemiology. We have therefore made an effort to identify bio-inspired paradigms that can be useful in DTNs, and have made an effort not only to map game theory to DTNs but also to create collaborations between game theory specialists and groups that specialize in DTNs within BIONETS.

We have studied two games. In [11] we considered a competition between two populations of nodes, each corresponding to a DTN network. The two networks are considered to compete over the delivery of a packet to a destination (whose location is not known). The problem is formulated as a stochastic game with a particular distributed structure that allows to fully solve it and to compute the equilibrium.

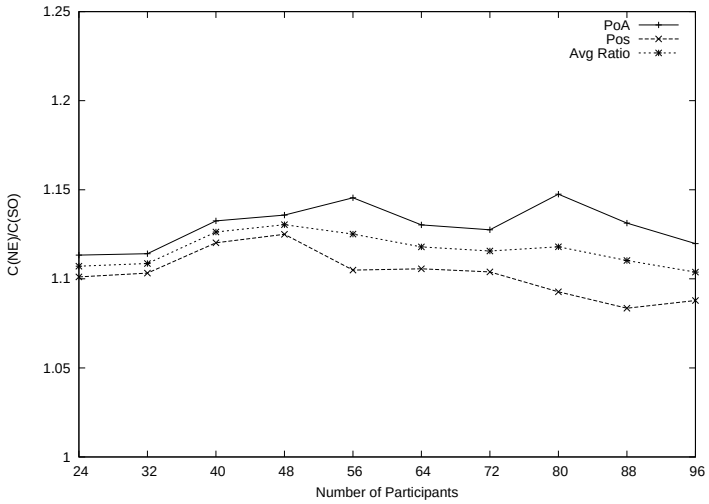

Figure 2: Evolution of PoS, PoA and average ratio with number of S-nodes.

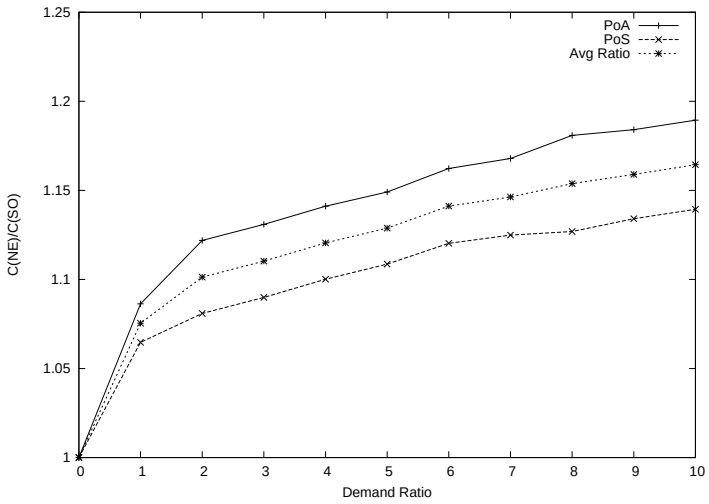

Figure 3: Evolution of PoS, PoA, and average coordination ratio (AVG) with demand ratio.

In [12] we consider a game where each mobile can decide whether to be active or not, or when to be active (e.g. how long to remain active). We call the first type of decision a "static" one and the second type a "dynamic" decision. The first mobile that delivers the packet to the destination receives one unit reward. Moreover, each mobile pays a cost of g per time unit that it is active. We show the existence of many equilibria and show how to achieve them [12].

3 Electromagnetism

3.1 Main results on magnetostatics

Various approaches inspired by physics have been proposed to deal with the routing problem in massively dense wireless sensor networks. Starting with the pioneering work of Jacquet (see [13, 14]) who used ideas

from geometrical optics to deal with the case of one source and one destination and a distribution of relay nodes.

Approaches based on electrostatics have been studied in [15, 16, 17, 18] (see the survey [19] and references therein) to deal with the case of a distribution of sources and a distribution of destinations with a distribution of relay nodes in a static environment.

Approaches based on road traffic theory have been studied in [20, 21, 22] defining the Wardrop equilibrium and a characterization of the Wardrop equilibrium in this type of setting and including a geometrical characterization of the flow of information based in some particular cost functions.

The development of the theory of routing in massively dense wireless sensor networks has emerged in a complete independent way of the theory developed within the community of road traffic engineers, introduced in 1952 by Wardrop [23] and Beckmann [24], see also [25, pp. 644, footnote 3] for the abundant literature of the early 50's, and which is still an active research area among that community, see [26, 27, 28, 29, 30] and references therein.

Consider that a spatially distributed set of mobile sources is creating data that must be delivered to a spatially distributed set of mobile sinks. In this context, our objective is to study the optimal traffic distribution and to find the minimum amount of relay nodes needed to transport the data over a wireless channel from the sources to the destinations.

The main contribution of this work is to address this problem from a mobile context where we analyze the cases where (i) only sources are mobile and the destinations are static as it would be in the case when the aggregation centers are fixed and the sensor nodes have the capability to move, (ii) the case when both sources and destinations are mobile, and given that the mathematics involve are similar (iii) we also analyze the case when the sources are static and the destinations are mobiles.

Definition.-[Divergence] Let x,y,z be a system of Cartesian coordinates on a 3-dimensional space and let $\hat{ß}, \hat{æ}$ and $\hat{k}$ be the corresponding basis of unit vectors respectively. The **divergence** of a continuously differentiable vector field $\mathbf{F} = F_x \hat{ß} + F_y \hat{æ} + F_z \hat{k}$ is defined to be the scalar-valued function:

$$\nabla \cdot \mathbf{F} = \frac{\partial F_x}{\partial x} + \frac{\partial F_y}{\partial y} + \frac{\partial F_z}{\partial z}.$$

An equivalent definition is the following: Given a sequence of surfaces A_k, that all include in their interior an arbitrary point (x_0, y_0, z_0), such that their areas $|A_k| \to 0$ with k, then

$$\nabla \cdot \mathbf{F}(x_0, y_0, z_0) = \lim_{k \to +\infty} \frac{1}{|A_k|} \int_{\partial A_k} \mathbf{F}(x,y,z) \cdot \mathbf{n}\, dV,$$

where $\mathbf{n}(\mathbf{x})$ is the unitary normal vector at $\mathbf{x}$.

We notice that both equivalent definitions can similarly be defined in a 2-dimensional Euclidean space.

Definition.-[Curl] Let x,y,z be a system of Cartesian coordinates on a 3-dimensional space and let $\hat{ß}, \hat{æ}$ and $\hat{k}$ be the corresponding basis of unit vectors respectively. The **curl** of a continuously differentiable vector field $\mathbf{F} = F_x \hat{ß} + F_y \hat{æ} + F_z \hat{k}$ is defined to be the vector field function:

$$\nabla \times \mathbf{F} = \left(\frac{\partial F_z}{\partial y} - \frac{\partial F_y}{\partial z} \right) \hat{ß} + \left(\frac{\partial F_x}{\partial z} - \frac{\partial F_z}{\partial x} \right) \hat{æ} + \left(\frac{\partial F_y}{\partial x} - \frac{\partial F_x}{\partial y} \right) \hat{k}.$$

Theorem.- [Divergence Theorem] The **divergence theorem** states that for any well-behaved vector field **A** defined within a volume V surrounded by the closed surface S the relation

$$\oint_S \mathbf{A} \cdot \mathbf{n}\, dS = \int_V \nabla \cdot \mathbf{A}\, dV$$

holds between the volume integral of the divergence of **A** and the surface integral of the outwardly directed normal component of **A**.

The same result holds in a 2-dimensional Euclidean space considering the corresponding definition of divergence.

Theorem.-[Stokes Theorem] The **Stokes theorem** states that if **A** is a well-behaved vector field, S is an arbitrary open surface and C is the closed curve bounding S, then

$$\oint_C \mathbf{A} \cdot d\ell = \int_S (\nabla \times \mathbf{A}) \cdot \mathbf{n}\, dS \tag{1}$$

where $\mathbf{n}(\mathbf{x})$ is the unitary normal vector at **x**.

3.2 Application to magnetons

Consider a network that contains mobile nodes on the line segment L. We first consider the one dimensional case and then we extend our result to the two dimensional case.

3.2.1 Fluid Approximations

Consider the continuous *node density function* $\eta(x)$, measured in nodes/m, as the fraction of mobile nodes at position x, defined so that the fraction of nodes in an area of infinitesimal size dA, centered at position x is equal to $\eta(x)\, dA$.

The total number of nodes on a region A, denoted by $N(A)$, will be

$$N(A) = \int_A \eta(x)\, dA.$$

Consider the continuous *information density function* $\rho(x)$, measured in bps/m, generated by the mobile sensor nodes such that

- At locations x where $\rho(x) > 0$ there is a fraction of data sources such that the rate with which information is created in an infinitesimal area of size dA, centered at position x is $\rho(x)\, dA$.
- Similarly, at locations x where $\rho(x) < 0$ there is a fraction of data destinations such that the rate with which information is absorbed by an infinitesimal area of size dA, centered at position x is equal to $-\rho(x)\, dA$.

We assume that the total rate at which sinks must absorb data is the same as the total rate which the data is created at the sources, *i.e.*

$$\int_L \rho(x)\, dA = 0. \tag{2}$$

Notice that if we have an estimation of the proportion of packet loss in the network, then we can tune our function ρ in order to adequate it to equation (2).

Consider the continuously differentiable *traffic flow function* $T(x)$, measured in bps/m, such that its direction (positive or negative) coincides with the direction of the flow of information at point x and $|T(x)|$ is the rate with which information propagates at position x, *i.e.* $|T(x)|$ gives the total amount of traffic that is passing at position x.

Next we present the flow conservation condition. For information to be conserved over a segment $[x_0, x_1]$ on the line L, it is necessary that the rate with which information is created in the area is equal to the rate with which information is leaving the segment, *i.e.*

$$T(x_1) - T(x_0) = \int_{x_0}^{x_1} \rho(x)\, dx$$

The integral on the right is equal to the quantity of information generated (if it's positive) or demanded (if it's negative) by the fraction of nodes in the segment $[x_0, x_1]$. The expression $T(x_1) - T(x_0)$, measured in bps/m, is equal at the rate with which information is leaving the segment $[x_0, x_1]$.

This holding for any segment, it follows that necessarily

$$\frac{dT(x)}{dx} = \rho(x). \tag{3}$$

Then the problem considered is to minimize the number of nodes in the line L needed to support the information created by the sources and received by the destinations subject to the flow conservation condition, *i.e.*

$$\text{Minimize } N(L)$$

subject to

$$\begin{array}{ll} \dfrac{dT(x)}{dx} & = \rho(x). \\ T(0) & = 0 \end{array}$$

Notice that in this case, last two equations have only one solution. We can suppose that the quantity of nodes in a region needed as relay nodes will be proportional to the traffic flow of information that is passing through that region, *i.e.* $\eta(x) = |T(x)|^{\alpha}$ where $\alpha > 0$. Then the total number of relay nodes needed to support the traffic flow function in the segment line will be

$$N(L) = \int_{x_0}^{x_1} \eta(x)\, dx = \int_{x_0}^{x_1} |T(x)|^{\alpha}\, dx.$$

Example 1.- Suppose that we can divide the segment line $[0, L]$ in two parts: (i) In $[0, L/2]$ there will be an uniform information density function generated by the sources of information given by $\rho(x) = 1$ bps/m and (ii) in $[L/2, L]$ there will be an uniform information density function received at the destinations given by $\rho(x) = -1$ bps/m. Then the traffic flow function will be given by $T(x) = x$ bps/m for all $x \in [0, L/2]$ and $T(x) = L - x$ bps/m for all $x \in [L/2, L]$ with positive direction. If we assume that $\alpha = 2$ in our model then the quantity of nodes needed to relay the information from the sources to the destinations will be given by $N(L) = \int_0^{L/2} x^2\, dx + \int_{L/2}^{L} (L-x)^2\, dx = L^3/12$.

3.2.2 The two dimensional case

Consider in the two dimensional plane[1] $X \times Y$ the continuous *information density function* $\rho(\mathbf{x})$, measured in bps$/$m^2, such that at locations $\mathbf{x}$ where $\rho(\mathbf{x}) > 0$ there is a distributed data source such that the rate with which information is created in an infinitesimal area of size dA centered at point $\mathbf{x}$ is $\rho(\mathbf{x})\,dA$. Similarly, at locations $\mathbf{x}$ where $\rho(\mathbf{x}) < 0$ there is a distributed data sink such that the rate with which information is absorbed by an infinitesimal area of size dA, centered at $\mathbf{x}$ is equal to $-\rho(\mathbf{x})\,dA$.

The total rate at which sinks must absorb data is the same as the total rate which the data is created at the sources, *i.e.*

$$\int_{X\times Y} \rho(\mathbf{x})\,dA = 0.$$

Consider the continuous *node density function* $d(\mathbf{x})$, measured in nodes$/$m^2, defined so that the number of nodes in an area of infinitesimal size dA, centered at $\mathbf{x}$ is equal to $d(\mathbf{x})\,dA$.

The total number of nodes on a region A, denoted by $N(A)$, is then given by

$$N(A) = \int_A d(\mathbf{x})\,dA.$$

Consider the continuous *traffic flow function* $\mathbf{T}(\mathbf{x})$, measured in bps$/$m, such that its direction coincides with the direction of the flow of information at point $\mathbf{x}$ and $\|\mathbf{T}(\mathbf{x})\|$ is the rate with which information crosses a linear segment perpendicular to $\mathbf{T}(\mathbf{x})$ centered on $\mathbf{x}$, *i.e.* $\|\mathbf{T}(\mathbf{x})\|\,\varepsilon$ gives the total amount of traffic crossing a linear segment of infinitesimal length ε, centered at $\mathbf{x}$ and placed vertically to $\mathbf{T}(\mathbf{x})$.

Next we present the flow conservation condition (see *e.g.* [16, 26] for more details). For information to be conserved over a domain D of arbitrary shape on the $X \times Y$ plane, with smooth boundary ∂D, it is necessary that the rate with which information is created in the area is equal to the rate with which information is leaving the area, *i.e.*

$$\int_D \rho(\mathbf{x})\,dD = \oint_{\partial D} [\mathbf{T}\cdot\mathbf{n}(\mathbf{x})]\,d\ell$$

The integral on the left is the surface integral of $\rho(\mathbf{x})$ over the domain D. The integral on the right is the path integral of the inner product $\mathbf{T}\cdot\mathbf{n}$ over the boundary ∂D. The vector $\mathbf{n}(\mathbf{x})$ is the unit normal vector to ∂D at the boundary point $\mathbf{x} \in \partial D$ and pointing outwards. Then the function $\mathbf{T}\cdot\mathbf{n}(\mathbf{x})$, measured in bps$/$m^2, is equal at the rate with which information is leaving the domain D at the boundary point $\mathbf{x}$.

This holding for any (smooth) domain D, it follows that necessarily

$$\nabla\cdot\mathbf{T}(\mathbf{x}) := \frac{\partial T_1(\mathbf{x})}{\partial x_1} + \frac{\partial T_2(\mathbf{x})}{\partial x_2} = \rho(\mathbf{x}), \tag{4}$$

where "$\nabla\cdot$" is the divergence operator.

Then the problem considered is to minimize the quantity of nodes in the smooth domain D needed to support the information created by the distribution of sources subject to the flow conservation condition, *i.e.*

$$\text{Minimize } N(D)$$
$$\text{subject to } \nabla\cdot\mathbf{T} = \rho(\mathbf{x}).$$

[1] We will denote with bold fonts the vectors and $\mathbf{x} = (x,y)$ will denote a point in the two dimensional space $X \times Y$.

Toumpis and Tassiulas in [15] focus on a particular physical layer model characterized by the following assumption:

Assumption 1: A location $\mathbf{x}$ where the node density is $d(\mathbf{x})$ can support any traffic flow vector with a magnitude less or equal to a bound $\|\mathbf{T}(\mathbf{x})\|_{max}$ which is proportional to the square root of the density, *i.e.* $\|\mathbf{T}(\mathbf{x})\| \leq \|\mathbf{T}(\mathbf{x})\|_{max} = K\sqrt{d(\mathbf{x})}$.

The validity of Assumption 1 depends on the physical layer and the medium access control protocol used by the network. Although it is not generally true, it holds in many different settings of interest. In [15] Toumpis and Tassiulas give an example of network where m^2 nodes are placed in a perfect square grid of $m \times m$ nodes and each node can listen to transmissions from its four nearest neighbors. They give a simple time division routine so that the network of m^2 nodes can support a traffic on the order of m.

As another example, in [32] it was shown that the traffic that can be supported in the above network, if nodes access the channel by use of slotted Aloha instead of time division, is $\mathbf{T}_{\text{local}} = K \times W \times m$, where nodes transmit data with a fixed global rate of W bps, K is a constant, smaller than $1/3$ that captures the efficiency of Aloha.

As another example, in [31] it was shown that a network of n randomly placed nodes can support an aggregate traffic on the order of $\sqrt{n/\log n}$ under a more realistic interference model that accounts for interference coming from arbitrarily distant nodes. The logarithm in the denominator appears due to the proving methodology of [31], and it has been shown [33] that it can be dispensed off, by use of percolation theory in the proofs.

Tassiulas and Toumpis prove in [15] that among all traffic flow functions that satisfy $\nabla \cdot \mathbf{T} = \rho$, the one that minimizes the number of nodes needed to support the network, must be irrotational, *i.e.*

$$\nabla \times \mathbf{T} = 0. \tag{5}$$

where "$\nabla\times$" is the curl operator.

For completeness let us prove this fact here.

Suppose that the traffic flow $\mathbf{T_0}$ that needs the minimum number of nodes has a non-zero curl at some point in the space.

An equivalent definition of the curl of a two dimensional vector field $\mathbf{T}$ at a point (x_1^0, x_2^0) is a scalar function defined as follows:

$$\nabla \times \mathbf{T} = \lim_{|A_k| \to 0} \frac{1}{|A_k|} \oint_{\partial A_k} \mathbf{T} \cdot d\ell,$$

where $\{A_k\}$ is a sequence of surfaces of vanishing area that contains (x_1^0, x_2^0) in their interior.

Then it follows that there is a curve C, of length L, along which the line integral of $\mathbf{T_0}$ is non-zero. Choosing a proper direction of C we can assume that the line integral is positive, i.e.

$$\oint_C \mathbf{T_0} \cdot d\ell = p > 0.$$

We can form around C a strip S of infinitesimal and constant width δ. As δ is infinitesimally small, the area of the strip can be taken to be equal to $|S| = \delta \cdot L$.

Consider an auxiliary vector function $\mathbf{T_1}$ such that outside the strip $\mathbf{T_1} = 0$, and inside the strip at a point (x_1, x_2), $\mathbf{T_1} = -\varepsilon\mathbf{t}$, where $\mathbf{t}$ is a unit vector tangential to C, at the point where C is closest to the point (x_1, x_2).

By the definition it is clear that $\mathbf{T_1}$ has a zero divergence everywhere. As the divergence operator is linear then

$$\nabla \cdot (\mathbf{T_0} + \mathbf{T_1}) = \nabla \cdot \mathbf{T_0} + \nabla \cdot \mathbf{T_1} = \rho.$$

Let N_0 be the total number of nodes needed to support $\mathbf{T_0}$ and N_{0+1} be the total number of nodes needed to support $\mathbf{T_0} + \mathbf{T_1}$. Then

$$\begin{aligned} N_0 - N_{0+1} &= \int_S (|\mathbf{T_0}|^2 - |\mathbf{T_0} + \mathbf{T_1}|^2) dS \\ &= \int_S (|\mathbf{T_0}|^2 - |\mathbf{T_0}|^2 - |\mathbf{T_1}|^2 - 2\mathbf{T_0} \cdot \mathbf{T_1}) dS \\ &= -\int_S \varepsilon^2 dS + \int_S 2\varepsilon \mathbf{T_0} \cdot \mathbf{t} dS \\ &= -\varepsilon^2 |S| + 2\varepsilon\delta \oint_C \mathbf{T_0} \cdot \mathbf{dl} \\ &= -\varepsilon^2 |S| + 2\varepsilon\delta p. \end{aligned}$$

It follows that for a sufficiently small value of ε, the traffic flow $\mathbf{T_0} + \mathbf{T_1}$ can be supported by a smaller number of nodes than the traffic flow $\mathbf{T_0}$. Therefore we arrive to a contradiction. Thus we conclude that $\nabla \times \mathbf{T} = 0$.

Notice that in the previous prove we never make any additional assumption about the time being fixed.

3.2.3 Model in movement

In our work we do a parallel to Electrodynamics by considering moving particles or moving distribution of particles. In that sense we first define some terms directly related to Electrodynamics. In our model, the functions ρ, $\mathbf{T}$, and d, defined previously may depend on time, *i.e.* $\rho = \rho(\mathbf{x}, t)$, $\mathbf{T} = \mathbf{T}(\mathbf{x}, t)$, and $d = d(\mathbf{x}, t)$, with $t \in [0, T)$.

We define the continuous *node current* $\mathbf{J}$ as the density of particles $\rho(\mathbf{x}, t)$ in the position $\mathbf{x}$ multiplied by the nodes average drift velocity $\mathbf{v}(\mathbf{x}, t)$, *i.e.*

$$\mathbf{J} = \rho(\mathbf{x}, t)\mathbf{v}(\mathbf{x}, t).$$

The rate at which nodes leaves an area (or volume) V, bounded by a curve (or surface) $S = \partial V$, will be given by

$$\oint_S \mathbf{J} \cdot dS \tag{6}$$

Since the quantity of nodes is conserved in the plane this integral must be equal to

$$-\frac{dN(S)}{dt} = -\int_V \frac{\partial \rho}{\partial t} dV. \tag{7}$$

From the divergence theorem and imposing the equality between the equations (6) and (7), we obtain the equivalent to Kirchhoff's current law:

$$\nabla \cdot \mathbf{J} + \frac{\partial \rho}{\partial t} = 0, \tag{8}$$

and as $\nabla \cdot \mathbf{J} = \nabla \cdot (\rho \mathbf{v}) = \mathbf{v} \cdot \nabla \rho + \rho \nabla \cdot \mathbf{v}$ and assuming that we have perfect knowledge of the initial distribution of the sources and sinks at time 0 denoted by ρ_0 we obtain the following system of equations:

$$(\mathrm{TE}) \begin{cases} \frac{\partial \rho}{\partial t} + \mathbf{v} \cdot \nabla \rho + \rho \nabla \cdot \mathbf{v} = 0 & \text{in } D \times (0,T) \\ \rho(0) = \rho_0 & \text{on } D \times \{0\} \end{cases}$$

which is a linear transport equation with initial condition for which there exists a solution from Proposition II.1 of [34].

Notice that given the initial distribution of the sources and sinks and the velocity of the distribution we are able to compute the evolution of the distribution of sources and sinks on time $t \in [0,T)$.

We recall that Tassiulas and Toumpis in [15] proved that among all traffic flow functions that satisfy $\nabla \cdot \mathbf{T} = \rho$, the one that minimize the number of nodes needed to support the network, must satisfy that $\nabla \times \mathbf{T} = 0$. Using Helmholtz's theorem (also known as fundamental theorem of vector calculus) in last equation we obtain that there exists a scalar potential function φ such that

$$-\nabla \varphi = \mathbf{T}. \tag{9}$$

Replacing this function into the conservation equation (3) we obtain that

$$-\Delta \varphi = \rho \tag{10}$$

and this holds for all $t \in [0,T)$.

We impose that no information is leaving the considered domain D, then $\mathbf{T} \cdot \mathbb{N} = 0$ and from equation (9) this condition translates into $\nabla \phi \cdot \mathbb{N} = 0$

From equation (10) and last condition we obtain the following system

$$(\mathrm{LP}) \begin{cases} -\Delta \varphi = \rho & \text{in } D \\ \nabla \varphi \cdot \mathbb{N} = 0 & \text{on } \partial D. \end{cases} \tag{11}$$

which is the *Laplace equation* with Neumann boundary conditions.

If the function f is square integrable then the Laplace equation with Neumann boundary conditions has a unique solution in $H^1(D)/\mathbb{R}$.

3.2.4 Numerical Results

Due to presentation effects we consider the one dimensional case during $T = 2$ hours.

We consider an initial distribution of the sources ρ_0^+ and an initial distribution of the sinks ρ_0^- on the positive real line $\mathbb{R}_+$ and we scale them to be probability distributions

$$\rho_0^+ = k_1 e^{-(x-3)^2} \quad \text{and} \quad \rho_0^- = -k_2 e^{-(x-10)^2}.$$

where $k_1 = \frac{2}{\sqrt{\pi}\mathrm{erfc}(-3)}$, $k_2 = \frac{2}{\sqrt{\pi}\mathrm{erfc}(-10)}$, and erfc(x) is the complementary error function defined as $\mathrm{erfc}(x) = \frac{2}{\sqrt{\pi}} \int_x^{+\infty} e^{-s^2} ds$.

We consider that the nodes average drift velocity is given by $v(x,t) = x$. The transportation equation then reads

$$\begin{cases} \frac{\partial \rho}{\partial t} + \frac{\partial (x\rho)}{\partial x} = 0 & \text{on } \mathbb{R}_+ \times [0,T) \\ \rho(0) = \rho_0^+ + \rho_0^- & \text{on } \mathbb{R}_+ \end{cases}$$

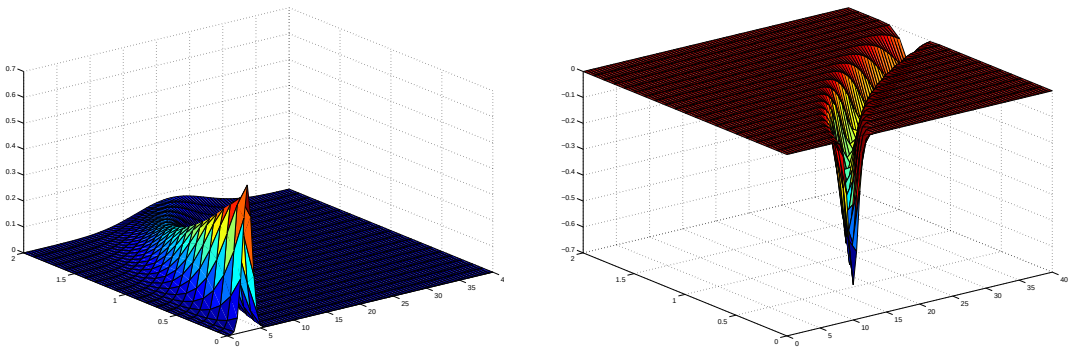

(a) (b)

Figure 4: Distribution of the sources (a) and destinations (b) information density.

Using the method of characteristics we obtain that the distribution of the information density function over time is given by

$$\rho(x,t) = \rho^+(x,t) + \rho^-(x,t)$$

where

$$\rho^+(x,t) = k_1 e^{-(xe^{-t}-3)^2-t} \quad \text{and} \quad \rho^-(x,t) = -k_2 e^{-(xe^{-t}-10)^2-t}.$$

The distribution of the sources and destinations information density function solution over time is showed in Figure 4.

From the conservation equation we obtain

$$\frac{\partial T(x,t)}{\partial x} = \frac{\partial T^+(x,t)}{\partial x} + \frac{\partial T^-(x,t)}{\partial x}$$

where

$$\frac{\partial T^+(x,t)}{\partial x} = \rho^+ \quad \text{and} \quad \frac{\partial T^-(x,t)}{\partial x} = -\rho^-.$$

with initial condition that the flow is zero at the boundary point zero, *i.e.* $T(0,t) = 0$.

Then the optimal traffic flow function is given by

$$T^*(x,t) = T^+(x,t) + T^-(x,t)$$

where

$$T^+(x,t) = \int_0^x k_1 e^{-(xe^{-t}-3)^2-t}\,dx \quad \text{and} \quad T^-(x,t) = -\int_0^x k_2 e^{-(xe^{-t}-10)^2-t}\,dx$$

And the minimal number of nodes needed to support the optimal flow at every time t will be given by

$$N(t) = \int_0^{+\infty} |T^*(x,t)|^2\,dx$$

3.2.5 Brownian Mobility Model

One of the most used mobility models used in networks is the Brownian Mobility Model [19].

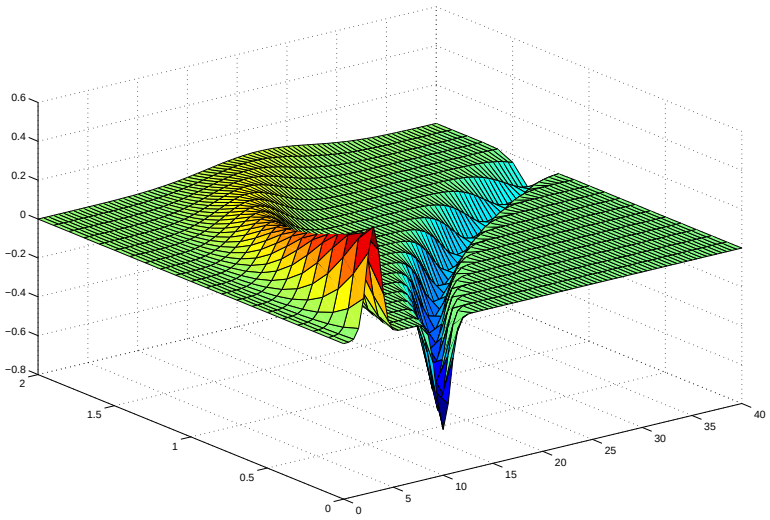

Figure 5: Distribution of the sources and destinations in the same line

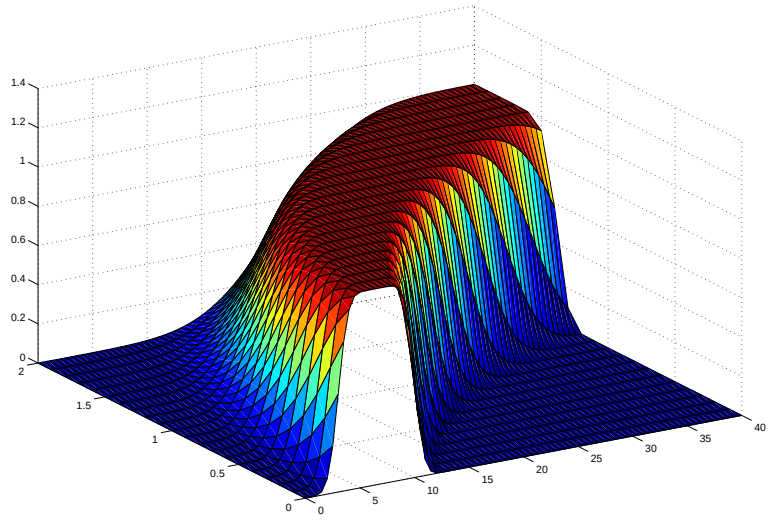

Figure 6: Optimal traffic flow

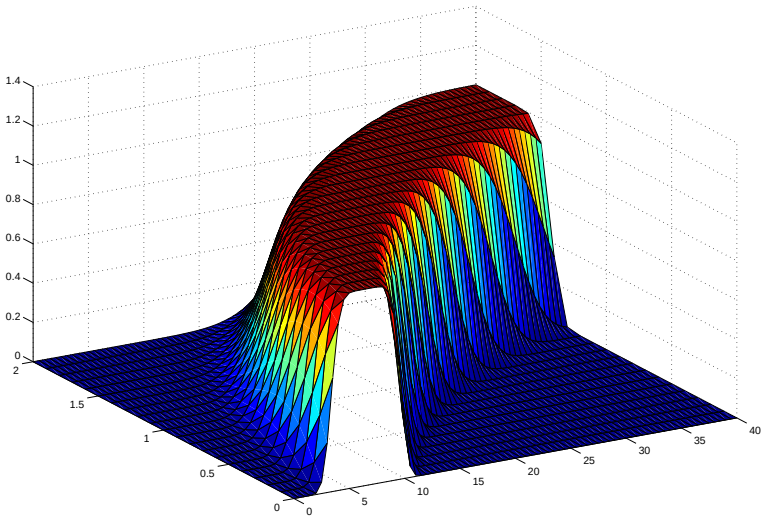

Figure 7: Optimal relay node distribution

If we have previous knowledge about the velocity drift of the distribution of sources (denoted ρ^+) and/or the distribution of the destinations (denoted ρ^-), and we assume the Brownian mobility model then the distribution of sources and/or the distribution of the destinations evolves according to the stochastic differential equation

$$d\rho^+(t) = \mathbf{v}^+(\mathbf{x},t)\,dt + \sigma_+(\mathbf{x},t)\,dW^+(t)$$

and/or

$$d\rho^-(t) = \mathbf{v}^-(\mathbf{x},t)\,dt + \sigma_-(\mathbf{x},t)\,dW^-(t).$$

where $W^+(t)$ and $W^-(t)$ are two independent Brownian motion with values in $X \times Y$.

Assuming as in the previous case that we know the initial distribution of the sources then by using Ito's lemma the distribution of the sources evolves in time by the Kolmogorov Forward Equation

$$\frac{\partial}{\partial s}p(x,s) = -\frac{\partial}{\partial x}[\mu(x,s)p(x,s)] + \frac{1}{2}\frac{\partial^2}{\partial x^2}[\sigma_+^2(x,s)p(x,s)].$$

for $s \geq 0$, with initial condition $p(x,0) = \rho^+(x)$

Equivalently, the initial distribution of the destinations evolves in time by the Kolmogorov Forward Equation

$$\frac{\partial}{\partial s}p(x,s) = -\frac{\partial}{\partial x}[\mu(x,s)p(x,s)] + \frac{1}{2}\frac{\partial^2}{\partial x^2}[\sigma_-^2(x,s)p(x,s)].$$

for $s \geq 0$, with initial condition $p(x,0) = \rho^-(x)$.

Example.- For the case where we do not have previous knowledge about the velocity drift then we just consider the standard Brownian mobility model given by

$$d\rho^+(t) = \sigma_+(\mathbf{x},t)\,dW^+(t)$$

and/or

$$d\rho^-(t) = \sigma_-(\mathbf{x},t)\,dW^-(t).$$

where $W^+(t)$ and $W^-(t)$ are two independent Brownian motions with values in $X \times Y$.

Then the previous equations translate into

$$\frac{\partial}{\partial s}p(x,s) = +\frac{1}{2}\frac{\partial^2}{\partial x^2}[\sigma_+^2(x,s)p(x,s)].$$

$$\frac{\partial}{\partial s}p(x,s) = +\frac{1}{2}\frac{\partial^2}{\partial x^2}[\sigma_-^2(x,s)p(x,s)].$$

which have as solution the following equations

$$\rho^+(x,t) = \frac{1}{\sqrt{2\pi t\sigma^+}}e^{-\frac{x^2}{2t\sigma^+}}$$

$$\rho^-(x,t) = \frac{1}{\sqrt{2\pi t\sigma^-}}e^{-\frac{x^2}{2t\sigma^-}}$$

Remark.- Notice that if we suppose that the distribution of the destinations is fixed, as it will be the case for aggregation centers of information, then $\sigma^- = 0$ and then $\rho^-(x,t) = \rho^-$ for all time t.

Finally replacing into the equation system (LP) we obtain a unique solution in $H^1(D)/\mathbb{R}$.

3.3 Hydrodynamics

We find in wikipedia the following definition:

> *In physics, fluid dynamics is a sub-discipline of fluid mechanics that deals with fluid flow-the natural science of fluids (liquids and gases) in motion. It has several sub-disciplines itself, including aerodynamics (the study of air and other gases in motion) and hydrodynamics (the study of liquids in motion).*

Our electromagnetic approach turned out to be one of the possible hydrodynamic modelling approaches. Indeed, just as the electrostatic approach, it allowed us to describe the continuum approximation of a system with finitely many particles (mobile terminals) as their number becomes large (and unlike the electrostatic approximation, it allows modelling the various aspects of mobility).

Within our collection of paradigms, we have also used equilibria notion taken from road traffic, namely the Wardrop equilibrium and its continuum limit. The Wardrop equilibrium can already be viewed as a hydrodynamic limit, as it regards each individual decision maker (a driver - in the road traffic context, and a mobile terminal - in networking) as an atom-less player, one of a continuum of players. Taking further the continuum limit of a network, as the number of links becomes large, extends the hydrodynamic approach to both time and space dimensions.

Both the road traffic approach as well as the electrostatic and electrodynamic paradigms have shown to be applicable in the context of massively dense ad hoc networks. This class of networks ended up not to be in the center of interest of the BIONETS project. Indeed, the project focused on systems operated in the sparse regime, which were closely related to so–called delay-tolerant networks. This class of networks, in contrast with the previously mentioned one, is characterized by intermittent connectivity among devices. Most work done on the modelling and optimization of such networks has been carried out using a mean

field limit that can be viewed as a hydrodynamic model. Optimization of the initial finite system turns out indeed to be rather hard to address in a closed-form way [11]. In [12], however, we show that the results obtained from the mean field approach represent the limit of those obtained for the discrete model, as the number of nodes grow to infinity. More details are presented in Sec. 2.4.

4 Statistical Physics

4.1 Theoretical results on Random Vandermonde Matrices

Analytical methods for finding moments of random Vandermonde matrices with entries on the unit circle are developed. Vandermonde Matrices play an important role in signal processing and wireless applications such as direction of arrival estimation, precoding or sparse sampling theory just to name a few. Within this framework, we extend classical freeness results on random matrices with i.i.d entries and show that Vandermonde structured matrices can be treated in the same vein with different tools. We focus on various types of Vandermonde matrices, namely Vandermonde matrices with or without uniformly distributed phase distributions, as well as generalized Vandermonde matrices (with non-uniform distribution of powers). In each case, we provide explicit expressions of the moments of the associated Gram matrix, as well as more advanced models involving the Vandermonde matrix. Comparisons with classical i.i.d. random matrix theory are provided and free deconvolution results are also discussed.

A Vandermonde matrix with entries on the unit circle has the following form

$$\mathbf{V} = \frac{1}{\sqrt{N}} \begin{pmatrix} 1 & \cdots & 1 \\ e^{-j\omega_1} & \cdots & e^{-j\omega_L} \\ \vdots & \ddots & \vdots \\ e^{-j(N-1)\omega_1} & \cdots & e^{-j(N-1)\omega_L} \end{pmatrix} \tag{12}$$

We will consider the case where ω_1,...,ω_L are independent and identically random variables taking values on $[0, 2\pi)$. Throughout the paper, the ω_i will be called *phase distributions*. Also, $\mathbf{V}$ will be used only to denote Vandermonde matrices with a given phase distribution, and the dimensions of the Vandermonde matrices will always be $N \times L$.

In many applications, N and L are quite large, and we may be interested in studying the case where both go to ∞ at a given ratio, with $\frac{L}{N} \to c$. The factor $\frac{1}{\sqrt{N}}$, as well as the assumption that the Vandermonde entries $e^{-j\omega_i}$ lie on the unit circle, are included in (12) to ensure that the analysis will give limiting asymptotic behaviour. Without this assumption, the problem at hand is more involved, since the rows of the Vandermonde matrix with the highest powers would dominate in the calculations of the moments for large matrices, and also grow faster to infinity than the $\frac{1}{\sqrt{N}}$ factor in (12), making asymptotic analysis difficult.

Remarkably, our results in this paper show that, asymptotically, the moments of the Vandermonde matrices depend only on the ratio c and the phase distributions, and have explicit expressions.

We will also extend our results to generalized Vandermonde matrices, i.e. matrices where the columns

do not consist of uniformly distributed powers. They are of the form

$$\mathbf{V} = \frac{1}{\sqrt{N}} \begin{pmatrix} e^{-j\lfloor Nf(0)\rfloor\omega_1} & \dots & e^{-j\lfloor Nf(0)\rfloor\omega_L} \\ e^{-j\lfloor Nf(\frac{1}{N})\rfloor\omega_1} & \dots & e^{-j\lfloor Nf(\frac{1}{N})\rfloor\omega_L} \\ \vdots & \ddots & \vdots \\ e^{-j\lfloor Nf(\frac{N-1}{N})\rfloor\omega_1} & \dots & e^{-j\lfloor Nf(\frac{N-1}{N})\rfloor\omega_L} \end{pmatrix}, \tag{13}$$

where f is called the power distribution, and is a function from $[0,1)$ to $[0,1)$. More general cases can also be considered, for instance by replacing f with a random variable λ, i.e.

$$\mathbf{V} = \frac{1}{\sqrt{N}} \begin{pmatrix} e^{-jN\lambda_1\omega_1} & \dots & e^{-jN\lambda_1\omega_L} \\ e^{-jN\lambda_2\omega_1} & \dots & e^{-jN\lambda_2\omega_L} \\ \vdots & \ddots & \vdots \\ e^{-jN\lambda_N\omega_1} & \dots & e^{-jN\lambda_N\omega_L} \end{pmatrix}, \tag{14}$$

with the λ_i mutually independent and distributed as λ, taking values in $[0,1)$, and also independent from the ω_j.

In the following, upper (lower boldface) symbols will be used for matrices (column vectors) whereas lower symbols will represent scalar values, $(.)^T$ will denote transpose operator, $(.)^\star$ conjugation and $(.)^H = \left((.)^T\right)^\star$ hermitian transpose. $\mathbf{I}_n$ will represent the $n \times n$ identity matrix. We let Tr be the (non-normalized) trace for square matrices, defined by,

$$Tr(\mathbf{A}) = \sum_{i=1}^{n} a_{ii},$$

where a_{ii} are the diagonal elements of the $n \times n$ matrix $\mathbf{A}$. We also let tr_n be the normalized trace, defined by $tr_n(\mathbf{A}) = \frac{1}{n} Tr(\mathbf{A})$.

Results in random matrix theory often refer to the empirical eigenvalue distribution of certain random matrices:

Definition 4.1 *With the empirical eigenvalue distribution of an $N \times N$ hermitian random matrix $\mathbf{T}$ we mean the (random) function*

$$F_{\mathbf{T}}^N(\lambda) = \frac{\#\{i|\lambda_i \leq \lambda\}}{N}, \tag{15}$$

where λ_i are the (random) eigenvalues of $\mathbf{T}$.

In the following, $\mathbf{D}_r(N), 1 \leq r \leq n$ will denote deterministic diagonal $L \times L$ matrices, where we implicitly assume that $\frac{L}{N} \to c$. We will assume that the $\mathbf{D}_r(N)$ have a joint limit distribution as $N \to \infty$ in the following sense:

Definition 4.2 *We will say that the $\{\mathbf{D}_r(N)\}_{1\leq r\leq n}$ have a joint limit distribution as $N \to \infty$ if the limit*

$$D_{i_1,\dots,i_s} = \lim_{N\to\infty} tr_L\left(\mathbf{D}_{i_1}(N)\cdots\mathbf{D}_{i_s}(N)\right) \tag{16}$$

exists for all choices of $i_1,\dots,i_s \in \{1,..,n\}$. For $\rho = \{W_1,\dots,W_k\}$, with $W_i = \{w_{i1},\dots,w_{i|\rho_i|}\}$, we also define

$$\begin{aligned} D_{W_i} &= D_{i_{w_{i1}},\dots,i_{w_{i|\rho_i|}}} \\ D_\rho &= \prod_{i=1}^{k} D_{W_i}. \end{aligned}$$

Although the matrices $\mathbf{D}_i(N)$ are assumed to be deterministic matrices throughout the paper, all presented formulas extend naturally to the case when $\mathbf{D}_i(N)$ are random matrices independent from the Vandermonde matrices. The difference when the $\mathbf{D}_i(N)$ are random is that covariances of traces come into play. $D_{\{\{1\},\{2,3\}\}}$ would for instance be

$$\lim_{N\to\infty} E\left[tr_L\left(\mathbf{D}(N)\right) tr_L\left(\left(\mathbf{D}(N)\right)^2\right)\right],$$

which is the covariance of two traces when $\mathbf{D}(N)$ is centered ($E[tr_L\mathbf{D}(N)] = 0$) and random.

Most theorems in this paper will present expressions for various mixed moments, defined in the following way:

Definition 4.3 *By a mixed moment we mean the limit*

$$\begin{array}{ll} M_n = \lim_{N\to\infty} E[tr_L(& \mathbf{D}_1(N)\mathbf{V}^H\mathbf{V}\mathbf{D}_2(N)\mathbf{V}^H\mathbf{V} \\ & \cdots \times \mathbf{D}_n(N)\mathbf{V}^H\mathbf{V})], \end{array} \tag{17}$$

whenever this exists.

A joint limit distribution of $\{\mathbf{D}_r(N)\}_{1\le r\le n}$ is always assumed in the presented results on mixed moments. A second type of mixed moments will also be considered, where several independent Vandermonde matrices are used instead of the diagonal matrices $\mathbf{D}_r(N)$. Note that when $\mathbf{D}_1(N) = \cdots = \mathbf{D}_n(N) = \mathbf{I}_L$, the M_n compute to the asymptotic moments of the Vandermonde matrices themselves, defined by

$$V_n = \lim_{N\to\infty} E\left[tr_L\left(\left(\mathbf{V}^H\mathbf{V}\right)^n\right)\right].$$

V_n corresponds also to the limit moments of the empirical eigenvalue distribution $F^N_{\mathbf{V}^H\mathbf{V}}$ defined by (15), i.e.

$$V_n = \lim_{N\to\infty} E\left[\int \lambda^n dF^N_{\mathbf{V}^H\mathbf{V}}(\lambda)\right].$$

Similarly, when $\mathbf{D}_1(N) = \cdots = \mathbf{D}_n(N) = \mathbf{D}(N)$, we will also write

$$D_n = \lim_{N\to\infty} tr_L(D(N)^n).$$

It will turn out that the following quantities are useful in describing limit distributions of Vandermonde matrices.

Definition 4.4 *Define*

$$\begin{array}{ll} K_{\rho,\omega,N} = & \frac{1}{N^{n+1-|\rho|}} \times \\ & \int_{(0,2\pi)^{|\rho|}} \prod_{k=1}^n \frac{1-e^{jN(\omega_{b(k-1)}-\omega_{b(k)})}}{1-e^{j(\omega_{b(k-1)}-\omega_{b(k)})}} \\ & d\omega_1\cdots d\omega_{|\rho|}, \end{array} \tag{18}$$

where $\omega_{W1},\ldots,\omega_{W_{|\rho|}}$ are i.i.d. (indexed by the blocks of ρ), all with the same distribution as ω, and where $b(k)$ is the block of ρ which contains k (where notation is cyclic, i.e. $b(-1) = b(n)$). If the limit

$$K_{\rho,\omega} = \lim_{N\to\infty} K_{\rho,\omega,N}$$

exists, then it is called a Vandermonde mixed moment expansion coefficient.

Our main result applies to Vandermonde matrices with any phase distribution. It restricts to the case when the expansion coefficients $K_{\rho,\omega}$ exist. Different versions of it adapted to different Vandermonde matrices will be also stated.

Theorem 4.1 *Assume that the $\{\mathbf{D}_r(N)\}_{1\leq r\leq n}$ have a joint limit distribution as $N\to\infty$. Assume also that all Vandermonde mixed moment expansion coefficients $K_{\rho,\omega}$ exist. Then the limit*

$$M_n = \lim_{N\to\infty} E[tr_L(\quad \mathbf{D}_1(N)\mathbf{V}^H\mathbf{V}\mathbf{D}_2(N)\mathbf{V}^H\mathbf{V} \\ \cdots\times\mathbf{D}_n(N)\mathbf{V}^H\mathbf{V})] \tag{19}$$

also exists when $\frac{L}{N}\to c$, and equals

$$\sum_{\rho\in\mathcal{P}(n)} K_{\rho,\omega}c^{|\rho|-1}D_\rho. \tag{20}$$

Next we derive and analyze the Vandermonde mixed moment expansion coefficients for the case of uniform phase distribution. It turns out that the non-crossing partitions play a central role for such matrices, but that the role is somewhat different than the relation for freeness. We will let u denote the uniform distribution on $[0,2\pi)$.

Proposition 4.1 *Assume that the $\{\mathbf{D}_r(N)\}_{1\leq r\leq n}$ have a joint limit distribution as $N\to\infty$, Then the Vandermonde mixed moment expansion coefficient*

$$K_{\rho,u} = \lim_{N\to\infty} K_{\rho,u,N}$$

exists for all ρ. Moreover, $0<K_{\rho,u}\leq 1$, the $K_{\rho,u}$ are rational numbers for all ρ, and $K_{\rho,u}=1$ if and only if ρ is non-crossing.

Following Proposition 4.1, we can obtain exact expressions for moments of lower order random Vandermonde matrices with uniform phase distribution, not only the limit, thus allowing for some finite-size systems analysis. The final result we address for the uniform phase distribution is the following:

Proposition 4.2 *The asymptotic mean eigenvalue distribution of a Vandermonde matrix with uniform phase distribution has unbounded support.*

The limit $K_{\rho,\omega}$ exists however for many ω, and also gives a useful expression for them in terms of the density of ω, and $K_{\rho,u}$.

Theorem 4.2 *The Vandermonde mixed moment expansion coefficients $K_{\rho,\omega}=\lim_{N\to\infty}K_{\rho,\omega,N}$ exist whenever the density p_ω of ω is continuous on $[0,2\pi)$. If this is fulfilled, then*

$$K_{\rho,\omega} = K_{\rho,u}(2\pi)^{|\rho|-1}\left(\int_0^{2\pi} p_\omega(x)^{|\rho|}dx\right). \tag{21}$$

An immediate consequence of this and Proposition 4.2 is that all phase distributions, not only uniform phase distribution, give Vandermonde matrices with unbounded mean eigenvalue distributions in the limit. Besides providing us with a deconvolution method for finding the mixed moments of the $\{\mathbf{D}_r(N)\}_{1\leq r\leq n}$, Theorem 4.2 also provides us with a way of inspecting the phase distribution ω, by first finding the moments

of the density, i.e. $\int_0^{2\pi} p_\omega(x)^k dx$. However, note that we can not expect to find the density of ω itself, only the density of the density of ω. To see this, define

$$Q_\omega(x) = \mu(\{x | p_\omega \leq x\})$$

for $0 \leq x \leq \infty$, where μ is uniform measure on the unit circle. Write also $q_\omega(x)$ as the corresponding density, so that $q_\omega(x)$ is the density of the density of ω. Then it is clear that

$$\int_0^{2\pi} p_\omega(x)^{|\rho|} dx = \int_0^{\infty} x^n q_\omega(x) dx. \tag{22}$$

These quantities correspond to the moments of the measure with density q_ω, which can help us obtain the density q_ω itself. However, the density p_ω can not be obtained, since we see that any reorganization of its values which do not change the density q_ω will provide the same values in (22). The asymptotics of Vandermonde matrices are different when the density of ω has singularities, and depends on the density growth rates near the singular points.

The asymptotics are first described for ω with atomic density singularities, as this is the simplest case to prove. After this, densities with polynomial growth rates near the singularities are addressed.

Theorem 4.3 *Assume that $p_\omega = \sum_{i=1}^r p_i \delta_{\alpha_i}$ is atomic (where $\delta_{\alpha_i}(x)$ is Dirac measure (point mass) at α_i), and denote by $p^{(n)} = \sum_{i=1}^r p_i^n$ the. Then*

$$\begin{aligned} \lim_{N\to\infty} \quad & E[Tr(\quad \mathbf{D}_1(N)\frac{1}{N}\mathbf{V}^H\mathbf{V}\mathbf{D}_2(N)\frac{1}{N}\mathbf{V}^H\mathbf{V} \\ & \qquad \cdots \times \mathbf{D}_n(N)\frac{1}{N}\mathbf{V}^H\mathbf{V})] \\ = \quad & \qquad c^{n-1}p^{(n)} \lim_{N\to\infty} \prod_{i=1}^n tr_L\left(\mathbf{D}_i(N)\right). \end{aligned}$$

Note here that the non-normalized trace is used.

In particular, Theorem 4.3 states that the asymptotic moments of $\frac{1}{N}\mathbf{V}^H\mathbf{V}$ coincide with the moments of p_ω, up to the scaling factor c^{n-1}.

The case when the density has non-atomic singularities is more complicated. We provide only the following result, which addresses the case when the density has polynomial growth rate near the singularities.

Theorem 4.4 *Assume that*

$$\lim_{x\to\alpha_i} |x-\alpha_i|^s p_\omega(x) = p_i \text{ for some } 0 < s < 1$$

for a set of points $\alpha_1, \ldots, \alpha_r$, with p_ω continuous for $\omega \neq \alpha_1, \ldots, \alpha_r$. Then

$$\begin{aligned} \lim_{N\to\infty} \quad & E[Tr(\quad \mathbf{D}_1(N)\frac{1}{N^s}\mathbf{V}^H\mathbf{V}\mathbf{D}_2(N)\frac{1}{N^s}\mathbf{V}^H\mathbf{V} \\ & \qquad \cdots \times \mathbf{D}_n(N)\frac{1}{N^s}\mathbf{V}^H\mathbf{V})] \\ = \quad & \qquad c^{n-1}q^{(n)} \lim_{N\to\infty} \prod_{i=1}^n tr_L\left(\mathbf{D}_i(N)\right) \end{aligned}$$

where

$$\begin{aligned} q^{(n)} &= \left(2\Gamma(1-s)\cos\left(\frac{(1-s)\pi}{2}\right)\right)^n p^{(n)} \times \\ &\int_{[0,1]^n} \prod_{k=1}^{n} \frac{1}{|x_{k-1}-x_k|^{1-s}} dx_1 \cdots dx_n, \end{aligned} \tag{23}$$

and $p^{(n)} = \sum_i p_i^n$. *Note here that the non-normalized trace is used.*

Further details with a look to possible applications are contained in [45].

4.2 Applications to node placement recovery

The distribution of randomly deployed wireless sensors plays an important role in the quality of the methods used for data acquisition and signal reconstruction. Mathematically speaking, the estimation of the distribution of randomly deployed sensors can be related to computing the spectrum of Vandermonde matrices with non-uniform entries. In this section, we use the recent free deconvolution framework to recover, in noisy environments, the asymptotic moments of the structured random Vandermonde matrices and relate these moments to the distribution of the randomly deployed sensors. Remarkably, the results are valid in the finite case using only a limited number of sensors and samples.

In the following, for simplicity sake and without loss of generality, we consider a one dimensional physical field with L sensors deployed in the interval $[0,1]$. Let $d_i \in [0,1]$ represent the position of the i^{th} sensor in the normalized interval. The continuous-time band-limited sensed signal $y(\omega_i)$ measured at the spatial position $\omega_i = 2\pi d_i$ can be represented as the weighted sum of P harmonics,

$$y(\omega_i) = \frac{1}{\sqrt{P}} \sum_{k=0}^{P-1} x_k e^{-jk\omega_i} \tag{24}$$

where $i = 1,2,\ldots,L$. x_k is the corresponding Fourier coefficients of the k^{th} harmonic. We suppose that the L samples are sent from the sensors to a common data-collecting unit through an orthogonal multiple access (TDMA for example) additive Gaussian noise channel. In this case, the model can be written in a vector form as:

$$\mathbf{y} = \mathbf{V}^H \mathbf{x} + \sigma \mathbf{n} \tag{25}$$

where $\mathbf{y}$ is the received signal vector of length L whose i^{th} element is $y(\omega_i)$, $\mathbf{x}$ is the transmitted signal of length P whose k^{th} element is x_k, $\mathbf{n}$ is the additive white Gaussian noise with unit variance noise vector of length L whereas σ^2 is the noise variance. $\mathbf{V}$ is a $P \times L$ Vandermonde matrix given by,

$$\mathbf{V} = \frac{1}{\sqrt{P}} \begin{pmatrix} 1 & \cdots & 1 \\ e^{-j\omega_1} & \cdots & e^{-j\omega_L} \\ \vdots & \ddots & \vdots \\ e^{-j(P-1)\omega_1} & \cdots & e^{-j(P-1)\omega_L} \end{pmatrix}. \tag{26}$$

Here $\omega_1, \omega_2, \ldots, \omega_L$ are i.i.d random variables with a certain distribution (related to the position of the sensors) and are bounded within the interval $[0, 2\pi)$. We suppose that we have K observations of the signal vector $\mathbf{y}$. In this case, the model takes the following matrix form:

$$\mathbf{Y} = \mathbf{V}^H\mathbf{X} + \sigma\mathbf{N} \tag{27}$$

Where $\mathbf{Y} = [\mathbf{y}_1, \mathbf{y}_2, \ldots, \mathbf{y}_K]$, $\mathbf{X} = [\mathbf{x}_1, \mathbf{x}_2, \ldots, \mathbf{x}_K]$ and $\mathbf{N} = [\mathbf{n}_1, \mathbf{n}_2 \ldots \mathbf{n}_K]$. The sample covariance matrix is defined as $\mathbf{YY}^H$.

In this section, we assume that the matrix $\mathbf{X}$ of unknown transmitted symbols and the noise matrix $\mathbf{N}$ are zero mean Gaussian matrices with i.i.d. entries of unit variance. Without loss of generality, we will consider $\sigma^2 = 1$. We will define the sample covariance associated with $\mathbf{Y}$ as $\mathbf{YY}^H$. Moreover, we will consider the asymptotic regime where $c_1 = \lim_{P\to\infty} \frac{P}{K}$, $c_2 = \lim_{P\to\infty} \frac{L}{P}$ and $c_3 = \lim_{K\to\infty} \frac{L}{K}$. Note that although L (number of sensors) and K are known (number of samples), P is unknown.

4.2.1 Distribution Estimation

The estimation of the distribution of ω in eq. (26) enables us to retrieve the distribution location of the sensors. In a blind context, with no training sequence and no communication between the sensors, this can be a hard task. However, as we will see afterwards, the moments of $\mathbf{VV}^H$ can be estimated and related to the distribution of the deployed sensors by using the moments approach. In particular, we relate the moments of $\mathbf{VV}^H$ up to a certain order with a polynomial approximation of the distribution of ω.

4.2.2 Step 1: Rectangular additive free deconvolution

Consider the covariance matrix

$$\mathbf{YY^H} = (\mathbf{A}+\mathbf{N})(\mathbf{A}+\mathbf{N})^H \tag{28}$$

where $\mathbf{A} = \mathbf{V}^H\mathbf{X}$. Rectangular additive free deconvolution ($\boxminus_{c_1}$) provides us with the moments of $\mathbf{YY^H}$ in terms of moments of $\mathbf{AA}^H$ and moments of $\mathbf{NN}^H$. In order to compute the series of moments, it turns out that it is much easier to compute cumulants. In free probability theory, the moments (m_n) are related to the sequence of numbers called the rectangular free cumulants (t_n) via the probability measure ε. [46] gives the following set of equations for the relation between the two.

$$T_\varepsilon(z(c_2 M_{\varepsilon^2}(z)+1)(M_{\varepsilon^2}(z)+1)) = M_{\varepsilon^2}(z)$$

where

$$T_\varepsilon(z) = \sum_{n\geq 1} t_n(\varepsilon) z^n \text{ and } M_{\varepsilon^2}(z) = \sum_{n\geq 1} m_n(\varepsilon) z^n.$$

This equation can be written in a recursive form as

$$\begin{aligned} m_0(\varepsilon) &= 1 \\ m_n(\varepsilon) &= t_n(\varepsilon) \\ &\quad + \sum_{k=1}^{n-1} c_1^k t_k(\varepsilon) \sum_{\substack{l_1,\ldots,l_{2k}\geq 0 \\ l_1+\ldots+l_{2k}=n-k}} m_{l_1}(\varepsilon)\ldots m_{l_{2k}}(\varepsilon) \end{aligned}$$

Let γ, η and τ be the probability measure of $\mathbf{YY}^H$, $\mathbf{AA}^H$ and $\mathbf{NN}^H$ respectively. In this case, these are related by [47]:

$$t_n(\eta) = t_n(\gamma) - t_n(\tau)$$

Note that as $\mathbf{N}$ is a random matrix with independent Gaussian entries with variance $\frac{1}{L}$ then the eigenvalue distribution of $\mathbf{N}\mathbf{N}^H$ follow a Marchenko-Pastur distribution with parameter $\frac{1}{c_3}$. In this case the rectangular free cumulants of $\mathbf{N}\mathbf{N}^H$ are given by [47] $t_n(\tau) = \delta_{n,1}$ [2], $\forall n \geq 1$.

Hence, the rectangular additive free deconvolution provides us with the moments of $\mathbf{V}^H\mathbf{X}\mathbf{X}^H\mathbf{V}$.

4.2.3 Step 2: Multiplicative free deconvolution

In this section, we show how one can extract the moments of $\mathbf{V}\mathbf{V}^H$ from $\mathbf{V}^H\mathbf{X}\mathbf{X}^H\mathbf{V}$. As a first step, note that:

$$m_n(\mathbf{X}\mathbf{X}^{\mathbf{H}}\mathbf{V}\mathbf{V}^H) = c_2 m_n(\mathbf{V}^H\mathbf{X}\mathbf{X}^H\mathbf{V}) \tag{29}$$

We can therefore use the concept of Multiplicative free deconvolution which computes the moments of $\mathbf{V}\mathbf{V}^H$ in terms of the moments of $\mathbf{X}\mathbf{X}^H\mathbf{V}\mathbf{V}^H$ and moments of $\mathbf{X}\mathbf{X}^H$. As previously, from an algorithmic perspective, it is easier to compute cumulants. The relationship between the moments m_n and the multiplicative free cumulants (s_n) is given by [45]:

$$M_\varepsilon(z)S_\varepsilon(M_\varepsilon(z)) = z(1+M_\varepsilon(z))$$

where,

$$S_\varepsilon(z) = \sum_{n\geq 1} s_n(\varepsilon)z^{n-1} \text{ and } M_\varepsilon(z) = \sum_{n\geq 1} m_n(\varepsilon)z^n.$$

These set of equations can be represented in a recursive form as

$$\begin{aligned} &m_1(\varepsilon)s_1(\varepsilon) = 1, \\ &m_n(\varepsilon) = \sum_{k=1}^{n+1} s_k(\varepsilon) \sum_{\substack{l_1,\ldots,l_k\geq 1 \\ l_1+\ldots+l_k=n+1}} m_{l_1}(\varepsilon)\ldots m_{l_k}(\varepsilon) \end{aligned}$$

Let ϑ, ς and ψ be the probability measures of $\mathbf{X}\mathbf{X}^H\mathbf{V}\mathbf{V}^H$, $\mathbf{X}\mathbf{X}^H$ and $\mathbf{V}\mathbf{V}^H$ respectively. Then these probability measures are related to each other thought the multiplicative free cumulants as

$$\begin{aligned} s_1(\varsigma)s_1(\psi) &= s_1(\vartheta) \\ s_1(\varsigma)s_n(\psi) &= s_n(\vartheta) - s_n(\varsigma)s_1(\psi) \\ &\quad - \sum_{k=2}^{n-1} s_k(\varsigma)s_{n+1-k}(\psi) \end{aligned}$$

Note that if $\mathbf{X}$ is a $P \times K$ random matrix with independent Gaussian entries with variance $\frac{1}{P}$ then the eigenvalue distribution of $\mathbf{X}\mathbf{X}^H$ follow a Marchenko-Pastur distribution with parameter $\frac{1}{c_1}$. In this case the multiplicative free cumulants of $\mathbf{X}\mathbf{X}^H$ are given by $s_n(\varsigma) = (-c_1)^{n-1}$, $\forall n \geq 1$.

[2] The Dirac delta function is defined as,

$$\delta_{n,1} = \begin{cases} 1 & \text{if } n = 1 \\ 0 & \text{else} \end{cases}$$

4.2.4 Step 3: Moments of $\mathbf{V}\mathbf{V}^H$

In the following, we assume that $\omega_i = 2\pi(i-1) + \omega_i'$ where $i = 1, 2, \ldots, L$. In other words, all the sensors are centered at equally spaced positions with a certain off-set. Here ω_i' is a random variable with continuous (not necessarily uniform) distribution and is bounded by $[0, 2\pi)$. We suppose that all ω_i' , $i = 1, 2, \ldots, L$ have the same distribution.

The asymptotic moments of the Vandermonde matrix are defined as

$$m_n = \lim_{P\to\infty} E[\mathrm{tr_P}(\mathbf{V}\mathbf{V}^{\mathrm{H}})^{\mathrm{n}}] \tag{30}$$

It has been shown recently in [45] that for any distribution of the random phases, the moments of the Vandermonde matrix can be calculated as

$$\sum_{\rho\in\mathcal{P}(n)} K_{\rho,\omega} c_2^{|\rho|} \tag{31}$$

where $\mathcal{P}(n)$ is the set of all partitions of $\{1, 2, \ldots, n\}$ and ρ is the notation for a particular partition in $\mathcal{P}(n)$. This can be also written as $\rho = \{\rho_1, \ldots, \rho_k\}$, where ρ_j are the blocks of ρ and $|\rho|$ is the number of blocks in ρ. $K_{\rho,\omega}$ are called the Vandermonde mixed moment expansion coefficient and are defined, in the case where ω is a uniform distribution $\omega \sim \mathcal{U}(0,1)^3$ as

$$K_{\rho,\omega} = \lim_{N\to\infty} \frac{1}{P^{n+1-|\rho|}} \int_{(0,2\pi)^{|\rho|}} \prod_{k=1}^{n} \frac{1 - e^{jP(\omega_{b(k-1)} - \omega_{b(k)})}}{1 - e^{j(\omega_{b(k-1)} - \omega_{b(k)})}} d\omega_1 \ldots d\omega_{|\rho|} \tag{32}$$

Interestingly, the moments of the Vandermonde matrix can be written in terms of the distribution of p_ω of ω as

$$m_n = \sum_{\rho\in\mathcal{P}(n)} K_{\rho,u} c_2^{|\rho|} I_{|\rho|} \tag{33}$$

where $I_{|\rho|} = (2\pi)^{|\rho|-1} \left(\int_0^{2\pi} p_\omega(x)^{|\rho|} dx \right)$ and $u \sim \mathcal{U}(0,1)$.

In general, it is extremely difficult to obtain an explicit expression of $K_{\rho,u}$ for any moments (in [45] only the first seven moments were computed). In this paper, we provide an algorithm to calculate all the moments:

Algorithm: $K_{\rho,u}$ can be expressed as the volume of the solution set of

$$\sum_{k\in\rho_j} l_{k-1} = \sum_{k\in\rho_j} l_k \tag{34}$$

with $0 \le l_k \le 1$. This volume is calculated after expressing $|\rho| - 1$ variables in terms of $n + 1 - |\rho|$ free variables and is bounded within $[0, 1]$. Note that $K_{\rho,u} = 1$ when the partitions of ρ are non-crossing [48] otherwise it is smaller the 1. As $I_{|\rho|}$ depends on the block cardinality $|\rho_j|$, we can therefore group together

[3] here $\mathcal{U}$ is the uniform distribution.

$K_{\rho,u}$ for ρ with equal block cardinality. Hence, we group the cardinality in descending order $r_1 \geq r_2 \geq \ldots \geq r_k$ and define

$$K_{r_1,r_2,\ldots,r_k} = \sum_{\hat{\rho}\in\mathcal{P}(n)} K_{\rho,u} \tag{35}$$

where $|\hat{\rho}_i| = r_i,\ \forall i$. In this case, the moments can be represented as

$$m_n = \sum_{k=1,2,\ldots,n} \sum_{\substack{r_1,r_2,\ldots,r_k \\ r_1+r_2+\cdots+r_k=n}} K_{r_1,r_2,\ldots,r_k} c_2^k I_k \tag{36}$$

As an example, the first moments expand to:

$$\begin{aligned} m_1 &= K_1 c_2 I_1 \\ m_2 &= K_2 c_2 I_1 + K_{1,1} c_2^2 I_2 \\ m_3 &= K_3 c_2 I_1 + K_{2,1} c_2^2 I_2 + K_{1,1,1} c_2^3 I_3 \\ m_4 &= K_4 c_2 I_1 + (K_{3,1} + K_{2,2}) c_2^2 I_2 + K_{2,1,1} c_2^3 I_3 \\ &\quad + K_{1,1,1,1} c_2^4 I_4 \\ \vdots &\quad \vdots \end{aligned} \tag{37}$$

4.2.5 Step 4: distribution Approximation

Now in order to estimate the distribution of ω, where ω is bounded within $[0,1)$, we use the Weierstrass approximation and multinomial expansion to derive an alternative form of I_n given by

$$\begin{aligned} I_n &= \lim_{t\to\infty} (2\pi)^{n-1} \sum_{k_1+\ldots+k_t=n} \binom{n}{k_1,\ldots,k_t} \\ &\quad \cdot \left(\frac{\Gamma(1+tn-\sum_{v=1}^{t} vk_v)\Gamma(\sum_{v=1}^{t} vk_v - n + 1)}{\Gamma((t-1)n+2)} \right) \\ &\quad \cdot \left(\prod_{v=1}^{t} \left[p_\omega\left(\frac{v-1}{t-1}\right) \binom{t-1}{v-1} \right]^{k_v} \right) \end{aligned} \tag{38}$$

where $p_\omega(x)$ represents the unknown distribution of ω and $p_\omega(0), p_\omega(\frac{1}{t-1}), p_\omega(\frac{2}{t-1}), \ldots, p_\omega(1)$ are the unknowns of the Weierstrass approximation. By equating (38) with (37), this will give us a set of non-linear equations to solve. As the number of unknowns should be equal to the number of equations, we take $n = t$. One can solve this by using any optimization algorithm.

4.3 Theoretical results on spiked random matrices with applications to node detection

Recent results on the analysis of spiked random matrix models are exploited to propose a new technique for collaborative sensing based on the analysis of the normalized (by the trace) maximum eigenvalues of the sample covariance matrix. Assuming that several base stations are cooperating and without the knowledge of the noise variance, the test is able to determine the presence of mobile users in a network when only few samples are available. Unlike previous heuristic techniques, we show that the test has roots within the Generalized Likelihood Ratio Test (GLRT) and provide an asymptotic random matrix analysis enabling to determine adequate threshold detection values (probability of false alarm). Simulations sustain the theoretical claims.

4.3.1 Signal Model

Consider a secondary wireless network formed by K nodes, working in sensing mode. We assume that all K nodes are simultaneously sensing a given sub-band $\mathcal{B}$ of the spectrum. For each $k = 1, \ldots, K$, we denote by $y_k(n)$ the complex envelope of the signal received by the kth sensor in band $\mathcal{B}$ after proper filtering and sampling. Denote by $\mathbf{y}(n) = [y_1(n), \ldots, y_K(n)]^T$ the vector obtained when stacking all K sensors' observations at time n into a column vector. The aim is to detect the presence of one or several primary transmitters in band $\mathcal{B}$. We respectively denote by H_0 and H_1 the hypotheses corresponding to the case where "band $\mathcal{B}$ is free" and "one or several primary devices are already transmitting in band $\mathcal{B}$":

$$\mathbf{y}(n) = \begin{cases} \mathbf{w}(n): & H_0 \mathbb{R} \\ \mathbf{H}\,\mathbf{s}(n) + \mathbf{w}(n): & H_1 \end{cases}, \tag{39}$$

where $\mathbf{w}(n)$ represents a complex circular temporally-white Gaussian noise vector with zero mean and covariance matrix equal to $\sigma^2 \mathbf{I}_K$. In the H_1-case, $\mathbf{s}(n) = [s_1(n), \ldots, s_P(n)]^T$ denotes the unknown P-dimensional process sent by the primary active devices. Integer P denotes the number of active transmitters in the band of interest. Sequence $\mathbf{s}(n)$ is assumed to be an independent identically distributed (i.i.d.) zero mean random sequence with independent entries. We assume without restriction that $s_p(n)$ has unit variance for each p. Matrix $\mathbf{H} \in \mathbb{C}^{K \times P}$ represents the complex-valued Multiple-Input Multiple-Output (MIMO) channel between the P transmitters and the K receiving nodes. In our context, most parameters are unknown. In particular:

- the noise variance σ^2 is unknown,
- the channel matrix $\mathbf{H}$ is unknown.

Depending on the context, the number of transmitters P may either be known or unknown. In case P is unknown, it is usually reasonable to assume that there exists a known integer P_{max} such that $P \leq P_{max} < K$. In that case, it is always possible to test hypothesis H_0 versus H_1, where P is replaced with P_{max}. In the sequel, we assume however that P is known.

we denote by N the number of samples observed by each sensor k. Consider the following $K \times N$ data matrix $\mathbf{Y}$:

$$\mathbf{Y} = [\mathbf{y}(0), \ldots, \mathbf{y}(N-1)]\,. \tag{40}$$

In order to test hypothesis H_0 versus H_1, the aim is to construct a relevant test function $\varphi : \mathbb{C}^{K \times N} \to \{0, 1\}$ with the sense that one decides hypothesis H_0 (resp. H_1) whenever $\varphi(\mathbf{Y}) = 0$ (resp. $\varphi(\mathbf{Y}) = 1$). As usual, we restrict ourselves to the search for test functions such that the probability of false alarm does not exceed a predefined threshold ε *i.e.*,

$$\mathbb{P}_{H_0}[\varphi(\mathbf{Y}) = 1] \leq \varepsilon\,, \tag{41}$$

where $\mathbb{P}_{H_0}[\mathcal{E}]$ represents the probability of a given event $\mathcal{E}$ under hypothesis H_0.

we investigate the case where input symbols $\mathbf{s}(\mathbf{n})$ are supposed to be Gaussian distributed: $\mathbf{s}(\mathbf{n}) \sim \mathcal{CN}(\mathbf{0}, \mathbf{I_P})$ where $\mathbf{I}_P$ denotes the $P \times P$ identity matrix. In this case, a generalized likelihood ratio test is likely to be implemented in order to decide H_0 *vs* H_1.

4.3.2 Likelihood Ratio

We respectively denote by $p_0(\mathbf{Y};\sigma^2)$ and $p_1(\mathbf{Y};\mathbf{H},\sigma^2)$ the likelihood functions of the observation matrix $\mathbf{y}$ indexed by the unknown parameters $\mathbf{H}$ and σ^2 under hypotheses H_0 and H_1 respectively:

$$p_0(\mathbf{Y};\sigma^2) = (\pi\sigma^2)^{-NK}\exp\left(-\frac{N}{\sigma^2}\operatorname{tr}\hat{\mathbf{R}}\right) \tag{42}$$

$$p_1(\mathbf{Y};\mathbf{H},\sigma^2) = (\pi^K\det\mathbf{R})^{-N}\exp\left(-N\operatorname{tr}\left(\hat{\mathbf{R}}\mathbf{R}^{-1}\right)\right) \tag{43}$$

where $\mathbf{R} = \mathbf{R}(\mathbf{H},\sigma^2)$ is the true covariance matrix under H_1 defined by

$$\mathbf{R} = \mathbf{H}\mathbf{H}^H + \sigma^2\mathbf{I}_K$$

and where $\hat{\mathbf{R}}$ is the sampled covariance matrix:

$$\hat{\mathbf{R}} = \frac{1}{N}\mathbf{Y}\mathbf{Y}^H.$$

In the ideal case where parameters $\mathbf{H}$ and σ^2 are supposed to be available, it is well known that a uniformly most powerful test rejects the null hypothesis when ratio

$$L_N(\mathbf{Y}) = \frac{p_0(\mathbf{Y};\sigma^2)}{p_1(\mathbf{Y};\mathbf{H},\sigma^2)}. \tag{44}$$

lies below a certain threshold which is selected so that (41) holds.

4.3.3 ML Estimates

The GLR is simply obtained by replacing the unknown parameter values $\mathbf{H}$ and σ^2 by their maximum likelihood (ML) estimates:

$$\hat{L}_N(\mathbf{Y}) = \frac{p_0(\mathbf{Y};\hat{\sigma}_0^2)}{p_1(\mathbf{Y};\hat{\mathbf{H}}_1,\hat{\sigma}_1^2)}. \tag{45}$$

where $\hat{\mathbf{H}}_1$ is the ML estimate of $\mathbf{H}$ under hypothesis H_1 and where $\hat{\sigma}_0^2$ (resp. $\hat{\sigma}_1^2$) is the ML estimate of σ^2 under hypothesis H_0 (resp. H_1). Denote by $\lambda_1 > \lambda_2 \cdots > \lambda_K \geq 0$ the ordered eigenvalues of $\hat{\mathbf{R}}$ (all distinct with probability one). For each $k = 1\ldots K$, denote by $\mathbf{e_k}$ the $K\times 1$ eigenvector associated with λ_k. The following Lemma provides the expression of the ML estimates $\hat{\sigma}_0^2$, $\hat{\sigma}_1^2$ and $\hat{\mathbf{H}}_1$. Note that the likelihood function is unchanged by right-multiplication of $\mathbf{H}$ with a $P\times P$ unitary matrix, thus $\mathbf{H}$ is identifiable only up to a unitary matrix.

Lemma 4.1 *ML estimates are given by:*

$$\begin{aligned}\hat{\sigma}_0^2 &= \frac{1}{K}\sum_{k=1}^{K}\lambda_k, \quad \hat{\sigma}_1^2 = \frac{1}{K-P}\sum_{k=P+1}^{K}\lambda_k \\ \hat{\mathbf{H}}_1 &= [\mathbf{e_1},\ldots,\mathbf{e_P}]\,diag\left(\sqrt{\lambda_1-\hat{\sigma}_1^2},\ldots,\sqrt{\lambda_P-\hat{\sigma}_1^2}\right)\mathbf{U}_P\end{aligned}$$

where $\mathbf{U}_P$ is a $P\times P$ unitary matrix indeterminacy.

The proof of the above lemma is omitted due to the lack of space. Using Lemma 4.1, we may now evaluate the GLR by substituting the values σ^2 and $\mathbf{R}$ in equations (42)-(43) with the corresponding ML estimates $\hat{\sigma}_0^2$ and $\hat{\mathbf{H}}_1\hat{\mathbf{H}}_1^H + \hat{\sigma}_1^2\mathbf{I}_K$ respectively. For each p, we define:

$$\mu_p = \frac{\lambda_p}{\frac{1}{K}\operatorname{tr}\hat{\mathbf{R}}}. \tag{46}$$

4.3.4 Proposed Hypothesis Test

The following result is a direct consequence of Lemma 1.

Proposition 4.3 *The GLR writes* $\hat{L}_N(\mathbf{Y}) = C \exp \mathcal{L}_N$ *where* $C = \left(1 - \frac{P}{K}\right)^{K-P}$ *is a constant and where* $\mathcal{L}_N = \mathcal{L}_N(\mu_1, \ldots, \mu_P)$ *is the statistic defined by*

$$\mathcal{L}_N = \sum_{p=1}^{P} \log \mu_p + (K-P) \log \left(1 - \frac{1}{K} \sum_{p=1}^{P} \mu_p \right). \tag{47}$$

The above result implies that the "trace-normalized" P largest eigenvalues $\mu_1, \ldots, \mu_P$ of the sampled covariance matrix form in some sense a sufficient statistic for the generalized likelihood ratio test. For technical reasons which will become clear in the sequel, we rather focus on the following "centered and rescaled" generalized log-likelihood ratio:

$$\bar{\mathcal{L}}_N = N^{2/3} \beta_N \left(\mathcal{L}_N - \alpha_N \right). \tag{48}$$

Here, we defined the centering constant α_N by

$$\alpha_N = 2P \log\left(1+\sqrt{c}\right) - P\left(1+\sqrt{c}\right)^2 \left(1 - \frac{P}{cN}\right) - \frac{P^2(1+\sqrt{c})^4}{2Nc} \tag{49}$$

and the normalisation constant β_N by

$$\beta_N = \frac{-(1+\sqrt{c})^{2/3}}{(2+\sqrt{c})\, c^{1/3}} \tag{50}$$

where we defined $c = K/N$.

4.4 Asymptotic Analysis

In the present section, we provide a simple procedure allowing to determine the threshold value, based on the asymptotic analysis of the test statistic $\bar{\mathcal{L}}_N$ under H_0. Our analysis is relevant in contexts where the number K of sensors is assumed to be large (*i.e.*, significantly larger than the number P of sources). Due to cognitive radio constraints, the secondary system must be able to decide the presence/absence of primary transmitters in a moderate amount of time. Therefore, we focus on the context where the number K of sensors and the number N of samples have the same order of magnitude. Otherwise stated, we consider the following asymptotic regime:

$$N \to \infty,\ K \to \infty,\ \ K/N \to c,\ \ P \text{ is fixed}, \tag{51}$$

where $0 < c < 1$ is a constant. It is worth stressing that under H_0, the distribution of $\mu_p = \lambda_p / (\frac{1}{K} \operatorname{tr} \hat{\mathbf{R}})$ does not depend on σ^2. Therefore, the distribution of $\bar{\mathcal{L}}_N$ does not depend on σ^2. As a consequence, there is no restriction in assuming that

$$\sigma^2 = 1$$

in the present section, for the sake of analysis.

4.4.1 Some Insights

The goal of the present section is to characterize the asymptotic behavior of $\bar{\mathcal{L}}_N$ as $N,K \to \infty$, under hypothesis H_0. In order to have some insights on this behavior, assume for the sake of illustration that $P = 1$ (at most one source is likely to be active).

Case $P = 1$. From Proposition 1, the (rescaled) generalized log-likelihood ratio $\bar{\mathcal{L}}_N$ is a function of the ratio $\mu_1 = \lambda_1/(\frac{1}{K}\operatorname{tr}\hat{\mathbf{R}})$. The asymptotic analysis of $\bar{\mathcal{L}}_N$ thus reduces to the separate study of λ_1 and $\frac{1}{K}\operatorname{tr}\hat{\mathbf{R}}$. First consider the largest eigenvalue λ_1 of $\hat{\mathbf{R}}$. Under hypothesis H_0, $\hat{\mathbf{R}}$ belongs to the Laguerre Unitary Ensemble (LUE). It is well known that λ_1 converges a.s. to the right edge of the Marchenko-Pastur distribution: $\lambda_1 \xrightarrow{a.s.} (1+\sqrt{c})^2$. A further result due to Johnstone (2001) states that convergence holds at speed $1/N^{2/3}$ and, more precisely, that the centered and rescaled quantity

$$\ell_1 = N^{2/3}\left(\frac{\lambda_1 - (1+\sqrt{c})^2}{(1+\sqrt{c})\left(\frac{1}{\sqrt{c}}+1\right)^{1/3}}\right) \tag{52}$$

converges in distribution toward a standard Tracy-Widom distribution function F_1 which can be defined in the following way:

$$F_1(s) = \exp\left(-\int_s^\infty (x-s)q^2(x)\,dx\right)\ , \tag{53}$$

where q solves the Painlevé II differential equation:

$$\begin{aligned} &q''(x) = xq(x) + 2q^3(x)\ , \\ &q(x) \sim \mathrm{Ai}(x) \quad \text{as} \quad x \to \infty \end{aligned}$$

and $\mathrm{Ai}(x)$ denotes the Airy function. This result provides the asymptotic behavior of the numerator λ_1 of μ_1.

Now consider the denominator $\frac{1}{K}\operatorname{tr}\hat{\mathbf{R}}$ of μ_1. By the law of large numbers, $\frac{1}{K}\operatorname{tr}\hat{\mathbf{R}}$ converges a.s. to $\sigma^2 = 1$. Furthermore, convergence holds at speed $1/N$ in the sense that $\frac{1}{K}\operatorname{tr}\hat{\mathbf{R}} = 1 + O_P(1/N)$ (where $O_P(1/N)$ stands for a term which is bounded in probability by C/N for a certain constant C). It is therefore straightforward to prove that ratio $\mu_1 = \lambda_1/(\frac{1}{K}\operatorname{tr}\hat{\mathbf{R}})$ has the same asymptotic behavior as λ_1. As a consequence, the asymptotic behavior of $\bar{\mathcal{L}}_N$ can be expressed in terms of the Tracy-Widom law (53).

Case $P > 1$. When the number P of sources is larger than one, a similar behavior occurs. In that case, the test statistics $\bar{\mathcal{L}}_N$ is a continuous function of $(\mu_1,\ldots,\mu_P)$ where for each $p = 1\ldots P$, $\mu_p = \lambda_p/(\frac{1}{K}\operatorname{tr}\hat{\mathbf{R}})$. Due to the same arguments, $(\mu_1,\ldots,\mu_P)$ has essentially the same asymptotic behavior as $(\lambda_1,\ldots,\lambda_P)$. Therefore, the asymptotic distribution of $\bar{\mathcal{L}}_N$ can be expressed in terms of the asymptotic joint distribution of the P largest eigenvalues $(\lambda_1,\ldots,\lambda_P)$ in the LUE. For each p, we define ℓ_p as the r.h.s. of equation (52) when λ_1 is replaced with λ_p. Random variables $(\ell_1,\ldots,\ell_P)$ are the properly centered and rescaled largest values of $\hat{\mathbf{R}}$.

We may now express the main result of the present section.

4.4.2 Main Result

Let $\xrightarrow{\mathcal{D}}$ denote the convergence in distribution in the asymptotic regime (51).

Theorem 4.5 *Under hypothesis H_0,*

$$\bar{\mathcal{L}}_N \xrightarrow{\mathcal{D}} \sum_{p=1}^{P} X_p \,, \tag{54}$$

where $(X_1,\ldots,X_P)$ follows a standard P-variate Tracy-Widom distribution.

Denote by $F_P(x)$ the distribution function of $\sum_p X_p$ and by F_P^{-1} the inverse of F_P w.r.t. composition.

Corollary 4.1 *Any threshold γ_N such that*

$$\gamma_N > F_P^{-1}(1-\varepsilon) \tag{55}$$

ensures that the probability of false alarm $\mathbb{P}_{H_0}[\bar{\mathcal{L}}_N < \gamma_N]$ is no larger than ε for N large enough.

We now make the following comments.

• The above results provide a simple way to set the threshold γ_N or to compute *p*-values associated with the proposed test. It prevents from using of tedious algorithms for approximating the distribution of $\bar{\mathcal{L}}_N$. Instead, it only relies on *pre-determined* tables of the distribution F_P. Such tables are well known in case $P = 1$. The case $P > 1$ has been subject to much less investigations at the present time (notice, however, that the main developments in the field of multivariate Tracy-Widom distributions are mostly very recent).

• Note that F_P does not depend on the technical parameters K, N or K/N. This observation is one of the main arguments for using test statistic $\bar{\mathcal{L}}_N$: the threshold selection procedure only depends on the desired probability of false alarm and on the maximum number of sources *P* likely to be present in a given band. It does not depend on the number of available snapshots. More importantly, it does not depend on the number of secondary users in the system. Such a flexibility of the test represents a particularly important feature for cognitive radio systems.

5 Relevance to BIONETS, Impact and Future Research

5.1 Relevance to BIONETS

The work presented in this deliverable included two major contributions to the BIONETS project. The first one relates to the development of appropriate tools for modelling BIONETS systems. The second one lies in the use of the modelling capabilities for optimization, and in particular for devising optimal control strategies, under both cooperative and non-cooperative (game theoretical) frameworks. The epidemic models and the magnetons used in Sections 2.1 and 3, respectively, provide modelling approaches that cover the two extreme networking situations (very dense vs. very sparse regimes) that can be encountered in BIONETS systems. In details:

- The epidemic models are useful for *sparse* networks with occasional connectivity (that occurs thanks to the mobility of the nodes).
- The magnetons allow us to study massively dense networks in which nodes relay traffic in a multi-hop fashion to reach far away destinations.

In both cases we may distinguish between intelligent nodes (which serve as gateways to the external Internet), and the other nodes (which are responsible for relaying information). Our study of Magnetons has provided the tools to model mobility of both types of nodes in the context of massively dense networks. For both cases, we have used the modelling approach to propose routing protocols that are based on hydrodynamic limits and have managed to relate them to the discrete case.

These modelling approaches, as well as the statistical physics approach based on the use of random matrix theory, present substantial advantages for system designers, as they allow to simplify considerably the computation burden involved in solving global optimisation or game problems. This is particularly true for the game problems, as games with an infinite number of players turn out to be much easier to solve than their finite counterpart.

5.2 Impact and Future Research

The adaptive, minimally co-ordinated interference-free co-existence of increasingly dense BIONETS-like systems is a research challenge and we have have shown how different methodologies inspired by physics paradigms enable the analysis of such systems.

The main impact of the work has been twofold:

- We were able to provide a systematic abstraction of the underlying physics and physical layer operation by identifying the system variables, typical topology classes and characteristic time-scales of system parameter variation. Our objective was to provide an an appropriate, tractable and realistic mathematical framework.
- In different cases, we were able to quantify the global network performance with respect to only the main variables of interest. This objective enabled us to assess the macroscopic performance of our proposed solutions objectively.

Unfortunately, much of the scientific background of this research rests on the probabilistic description of a large-scale wireless network. Significant extensions of the established techniques are required in order to both optimize and regulate the operation of such networks in a systematic and mathematically well-founded manner. This requires developments in two distinct areas of science: probabilistic inference and game theory (that have been tackled within the project).

Traditional probabilistic inference assigns different mathematical tools to problems that fall clearly into the following regimes: (a) conventional optimization methods apply to systems with continuous variables; (b) probabilistic message passing methods are used to tackle systems with discrete sparsely interacting variables; (c) mean field-like approaches are employed for systems of densely interacting variables. In order to tackle the proposed wireless networking problem **we need to extend the above techniques to cope with near-sparse systems of both discrete and continuous variables**. This condition can also be viewed through a Physics analogy as it relates to percolation theory: At one extreme, when nodes adopt a high transmission power, interaction (interference) is strong and changing one transmission parameter (e.g. frequency of operation) will have a knock-on effect that ripples throughout the network. At the other extreme, low transmission powers can result in a network that is fragmented into islands of mutually interfering nodes where changing one transmission parameter will only have a localized, limited effect on

neighbours. The transition between the two phases is termed the percolation threshold, and we have only operated beyond that mode (assuming only a dense wireless environment and not a mixture of the two).

Game theory has been already applied to a number of networking problems (including game-theoretic MAC protocols), but always under the condition that each node is explicitly “aware” of all other neighboring, competing nodes. The foundations of game theory should be extended to include the inference of other hidden players and more importantly an estimate of their operational states to rationally enforce fairness.

References

[1] M. Benaim and J. Y. Le Boudec, *A Class Of Mean Field Interaction Models for Computer and Communication Systems*, Performance Evaluation, 2008.

[2] M. Benaim and J. W. Weibull *Deterministic Approximation of Stochastic Evolution in Games*, Econometrica 71, 873-903, 2003.

[3] W. H. Sandholm, *Population Games and Evolutionary Dynamics*, to appear MIT Press, 2009.

[4] H. Tembine, E. Altman , R. ElAzouzi, W. H. Sandholm , *Evolutionary game dynamics with migration for hybrid power control in wireless communications*, in Proc. of 47th IEEE Conference on Decision and Control (CDC), 2008.

[5] H. Tembine, J. Y. Le Boudec, R. El-Azouzi, E. Altman, *Mean Field Asymptotic of Markov decision evolutionary games*, International IEEE Conference on Game Theory for Networks, Gamenets 2009

[6] H. Tembine, E. Altman, R. El-Azouzi and Y.Hayel, "Stochastic Population Games with individual independent states and coupled constraints", In the proceeding of valuetools 20-24 October, Athens, Greece, 2008

[7] H. Tembine, J. Y. Le Boudec, R. El-Azouzi and E. Altman, "From mean field interaction to evolutionary game dynamics" PHYSCOMNET’09, June 27th, 2009, Seoul, Korea.

[8] E. Altman, Y. Hayel, H. Tembine, R. El-Azouzi, "Markov decision Evolutionary Games with Time Average Expected Fitness Criterion", In proc. of Valuetools, October, 2008.

[9] Tanabe Y., The propagation of chaos for interacting individuals in a large population, Mathematical Social Sciences, 2006,51,2,pp.125-152.

[10] G. Y. Weintraub, L. Benkard, B. Van Roy, Oblivious Equilibrium: A mean field Approximation for Large- Scale Dynamic Games, Advances in Neural Information Processing Systems, Vol 18, 2006.

[11] Eitan altman, Giovanni Neglia, Francesco De Pellegrini, Daniele Miorandi. "Decentralized Stochastic Control of Delay Tolerant Networks", IEEE Infocom, Rio de Janeiro, Brazil, April 19-25, 2009

[12] E. Altman, Competition and cooperation between nodes in Delay Tolerant Networks with Two Hop Routing, proceedings of NetCoop 2009.

[13] P. Jacquet, "Geometry of information propagation in massively dense ad hoc networks," in *Proc. of MobiHoc '04: Proceedings of the 5th ACM international symposium on Mobile ad hoc networking and computing*, pp. 157–162, New York, NY, USA, 2004.

[14] P. Jacquet, "Space-Time Information Propagation in Mobile Ad-hoc Wireless Networks," *IEEE Information Theory Workshop*, pp. 260–264, 2004.

[15] S. Toumpis and L. Tassiulas, "Packetostatics: Deployment of Massively Dense Sensor Networks as an Electrostatic Problem," *IEEE INFOCOM*, Vol. 4, pp. 2290–2301, 2005.

[16] S. Toumpis and L. Tassiulas, "Optimal Deployment of Large Wireless Sensor Networks," *IEEE Trans. on Information Theory*, Vol. 52, No. 7, pp. 2935–2953, Jul. 2006.

[17] S. Toumpis and G. A. Gupta, "Optimal Placement of Nodes in Large Sensor Networks under a General Physical Layer Model" in *Proc. of IEEE SECON* 2005.

[18] R. Catanuto, G. Morabito, and S. Toumpis, "Optical Routing in Massively Dense Networks: Practical Issues and Dynamic Programming Interpretation." *IEEE International Symposium on Wireless Communication Systems*, Valencia, Spain, Sep. 2006.

[19] S. Toumpis, "Mother Nature Knows Best: A Survey of Recent Results on Wireless Networks Based on Analogies with Physics," *Computer Networks*, Vol. 52, No. 2, pp. 360–383, Feb. 2008.

[20] E. Altman, A. Silva, P. Bernhard, M. Debbah, "Continuum Equilibria for Routing in Dense Ad-Hoc Networks," 45th Allerton Conference on Communication, Control and Computing, Illinois, USA, Sep. 26-28, 2007.

[21] E. Altman, P. Bernhard, A. Silva, "The Mathematics of Routing in Massively Dense Ad-Hoc Networks," *Proc. of AdHoc-NOW Conference*, Sophia-Antipolis, France, Sep. 10-13, 2008.

[22] A. Silva, P. Bernhard, E. Altman, "Numerical Solutions of Continuum Equilibria for Routing in Dense Ad-hoc Networks," *Proc. of Valuetools*, Workshop Inter-Perf, Athens, Greece, Oct. 20-24, 2008.

[23] J.G. Wardrop, "Some theoretical aspects of road traffic research," *Proceedings of the Institution of Civil Engineers*, Part II, I:325–378, 1952.

[24] M. Beckmann, "A continuum model of transportation," *Econometrica* Vol. 20, pp. 643-660, 1952.

[25] M. Beckmann, C. B. McGuire and C. B. Winsten, *Studies in the Economics and Transportation*, Yale Univ. Press, 1956.

[26] S. C. Dafermos, "Continuum Modeling of Transportation Networks," *Transportation Research* Vol. 14B, pp. 295–301, 1980.

[27] P. Daniele and A. Maugeri, "Variational Inequalities and discrete and continuum models of network equilibrium protocols," *Mathematical and Computer Modelling* 35:689–708, 2002.

[28] H.W. Ho and S.C. Wong, "A Review of the Two-Dimensional Continuum Modeling Approach to Transportation Problems," *Journal of Transportation Systems Engineering and Information Technology*, Vol.6 No.6 P.53–72, 2006.

[29] G. Idone, "Variational inequalities and applications to a continuum model of transportation network with capacity constraints," *Journal of Global Optimization* 28:45–53, 2004.

[30] S.C.Wong, Y.C.Du, J.J.Sun and B.P.Y.Loo, "Sensitivity analysis for a continuum traffic equilibrium problem," *Ann Reg Sci* 40:493–514,, 2006.

[31] P. Gupta and P. Kumar, "The capacity of wireless networks," *IEEE Transactions on Information Theory*, Vol. IT-46, No. 2, pp. 388–404, Mar. 2000.

[32] J. Silvester and L. Kleinrock, "On the capacity of multihop slotted ALOHA networks with regular structures," *IEEE Trans. Commun.*, Vol. 31, No. 8, pp. 974–982, Aug. 1983.

[33] M. Franceschetti, O. Dousse, D. Tse, and P. Tiran, "Closing the gap in the capacity of random wireless networks," in *Proc. of IEEE ISIT* 2004.

[34] R. J. Di Perna and P. L. Lions "Ordinary differential equations, transport theory and Sobolov spaces," *Inventiones mathematicae*, Vol. 98, pp. 511–547, 1989.

[35] G. Carlier and A. Lachapelle, "Optimal Transportation and optimal control in a finite horizon framework," *To appear*.

[36] E. Anshelevich, A. Dasgupta, J. M. Kleinberg, E. Tardos, T. Wexler, and T. Roughgarden. The Price of Stability for Network Design with Fair Cost Allocation. In *Proceedings of IEEE Annual Symposium on Foundations of Computer Science (FOCS)*, pages 295–304, 2004.

[37] E. Anshelevich, A. Dasgupta, E. Tardos, and T. Wexler. Near-optimal network design with selfish agents. In *Proceedings of the ACM Annual Symposium on Theory of Computing (STOC)*, pages 511–520, 2003.

[38] E. Koutsoupias and C. H. Papadimitriou. Worst-case Equilibria. In *Proceedings of the Symposium on Theoretical Aspects of Computer Science (STACS)*, pages 404–413, 1999.

[39] N. Laoutaris, O. A. Telelis, V. Zissimopoulos, and I. Stavrakakis. Distributed Selfish Replication. *IEEE Transactions on Parallel and Distributed Systems*, 17(12):1401–1413, 2006.

[40] Avraham Leff, Joel L. Wolf, and Philip S. Yu. Replication algorithms in a remote caching architecture. *IEEE Transactions on Parallel and Distributed Systems*, 4(11):1185–1204, 1993.

[41] M. J. Osborne and A. Rubinstein. *A course in game theory*. MIT Press, 1994.

[42] Gerasimos G. Pollatos, Orestis Telelis, and Vassilis Zissimopoulos. On the social cost of distributed selfish content replication. In *7th International IFIP-TC6 Networking Conference*, pages 195–206, 2008.

[43] M. R. Garey, D. S. Johnson. *Computers and Intractability: A Guide to the Theory of NP-Completeness*. W. H. Freeman, 1979.

[44] Chun, B., Chaudhuri, K., Wee, H., Barreno, M., Papadimitriou, C.H., Kubiatowicz, J.: Selfish caching in distributed systems: a game-theoretic analysis. In: Proceedings of the ACM Symposium on Principles of Distributed Computing (PODC). (2004)

[45] Ø. Ryan and M. Debbah "Asymptotic Behaviour of Random Vandermonde Matrices with Entries on the Unit Circle," IEEE Transactions on Information Theory, V. 55, nr. 7 pages.

[46] F. Benaych-Georges and M. Debbah "Free Deconvolution: from Theory to Practice," submitted to *IEEE Trans. on Information Theory*, 2008

[47] F. Benaych-Georges "Infinitely divisible distribution for rectangular free convolution: classification and matricial interpretation," *Probab. Theory Related Fields*, vol. 139, no. 1-2, pp. 143-189, 2007.

[48] R. Speicher "Free Probability Theory and Non-Crossing partitions," *Séminaire Lotharingien de Combinatoire*, B39c (1997), 38 pages, 1997.

Appendices

A Worst-case equilibria for the S-nodes reconfiguration game.

As stated previously, the price of anarchy is essentially a measure of efficiency of the achieved pure equilibria of a strategic game. In order to bound in the worst-case this ratio we must assume that all players (S-nodes) have a *marginal* interest in participating in the subnetwork of S-nodes, expressed by $|R_i| \geq cap_i$. If this does not hold, then equilibria may be unboundedly inefficient, because of unused storage space in certain S-nodes.

In what follows, we compare a worst-case socially most expensive equilibrium placement X towards the socially optimum placement X^*, and use $d_i(\cdot)$ and $d_i^*(\cdot)$ for minimum communication costs for fetching data objects in each placement. The analysis is performed for the individual cost $c_i(X) = -b_i(X)$ of a single fixed S-node i.

Lemma A.1 *If X and $X^\star$ are equilibrium and optimum placements respectively, for each S-node i we have:*

$$c_i(X) = \sum_{o \in R_i \setminus (P_i \cup P_i^\star)} w_i(o) d_i(o) + \sum_{o \in P_i^\star \setminus P_i} w_i(o) d_i(o) \tag{56}$$

$$c_i(X^\star) = \sum_{o \in R_i \setminus (P_i^\star \cup P_i)} w_i(o) d_i^\star(o) + \sum_{o \in P_i \setminus P_i^\star} w_i(o) d_i^\star(o) \tag{57}$$

Proof: By noticing that:

$$R_i \setminus P_i = (R_i \setminus (P_i \cup P_i^\star)) \cup (P_i^\star \setminus P_i) \text{ and } (R_i \setminus (P_i \cup P_i^\star)) \cap (P_i^\star \setminus P_i) = \emptyset$$

$$R_i \setminus P_i^\star = (R_i \setminus (P_i^\star \cup P_i)) \cup (P_i \setminus P_i^\star) \text{ and } (R_i \setminus (P_i^\star \cup P_i)) \cap (P_i \setminus P_i^\star) = \emptyset$$

yields the result. ■

The following lemma associates access costs for two distinct objects in respect to a socially optimum placement:

Lemma A.2 *If X and $X^\star$ are equilibrium and optimum placements respectively, for every player (S-node) i we have that $|P_i \setminus P_i^\star| = |P_i^\star \setminus P_i|$ and for every pair of objects $o \in P_i \setminus P_i^\star$, $o' \in P_i^\star \setminus P_i$ it is $w_i(o)d_i(o) \geq w_i(o')d_i(o')$.*

Proof: Since for every player i $cap_i < |R_i|$, we obtain $|P_i \setminus P_i^\star| = |P_i^\star \setminus P_i|$. For every pair of objects $o \in P_i \setminus P_i^\star$, $o' \in P_i^\star \setminus P_i$ it must be $w_i(o)d_i(o) > w_i(o')d_i(o')$, for otherwise, player i would have an incentive to unilaterally deviate in placement X, by substituting o for o', thus decreasing its individual access cost. ■

Thus, for the value of the Price of Anarchy we conclude that:

Theorem A.1 *The price of anarchy is upper bounded by $\frac{d_{max}}{d_{min}}$, where d_{max} is the maximum communication cost among the S-nodes and d_{min} the minimum one.*

Proof: Starting from expression (57) and using lemma A.2 we have:

$$\begin{aligned} c_i(X^\star) &= \sum_{o \in R_i \setminus (P_i^\star \cup P_i)} w_i(o) d_i^\star(o) + \sum_{o \in P_i \setminus P_i^\star} w_i(o) d_i^\star(o) \\ &\geq \sum_{o \in R_i \setminus (P_i^\star \cup P_i)} w_i(o) d_i^\star(o) \frac{d_i(o)}{d_i(o)} + \sum_{o' \in P_i^\star \setminus P_i} w_i(o') \frac{d_i(o')}{d_i(o)} d_i^\star(o) \\ &\geq \sum_{o \in R_i \setminus (P_i^\star \cup P_i)} w_i(o) d_i(o) \frac{d_{min}}{d_{max}} + \sum_{o' \in P_i^\star \setminus P_i} w_i(o') d_i(o') \frac{d_{min}}{d_{max}} \end{aligned}$$

By expression (56) $c_i(X^\star) \geq \frac{d_{min}}{d_{max}} c_i(X)$. Summing over all i yields the result. ■